

The phase diagram of dense QCD

Kenji Fukushima¹ and Tetsuo Hatsuda²

¹ Yukawa Institute for Theoretical Physics, Kyoto University, Oiwake-cho, Kitashirakawa, Sakyo-ku, Kyoto-shi, Kyoto 606-8502, Japan

² Department of Physics, The University of Tokyo, 7-3-1 Hongo, Bunkyo-ku, Tokyo 113-0033, Japan

E-mail: fuku@yukawa.kyoto-u.ac.jp

E-mail: hatsuda@phys.s.u-tokyo.ac.jp

Abstract. Current status of theoretical researches on the QCD phase diagram at finite temperature and baryon chemical potential is reviewed with special emphasis on the origin of various phases and their symmetry breaking patterns. Topics include; quark deconfinement, chiral symmetry restoration, order of the phase transitions, QCD critical point(s), colour superconductivity, various inhomogeneous states and implications from QCD-like theories.

Submitted to: *Rep. Prog. Phys.*

Contents

1	Introduction	2
2	QCD phase structure	3
2.1	Deconfinement and chiral restoration	4
2.2	Conjectured QCD phase diagram	5
3	Order parameters for the QCD phase transition	8
3.1	Polyakov loop and quark deconfinement	8
3.2	Chiral condensate and dynamical breaking of chiral symmetry	10
3.3	Diquark condensate and colour superconductivity	11
4	Chiral phase transition at finite temperature	11
4.1	Ginzburg-Landau-Wilson analysis	11
4.2	Lattice QCD simulations	13
5	Chiral phase transition at finite baryon density	14
5.1	Lattice QCD at low baryon density	15
5.2	Effective $U(1)_A$ symmetry restoration	19
5.3	QCD critical point search	20
5.4	First-order phase transition at high baryon density	21
6	Formation of the diquark condensate	23
6.1	Neutrality in electric and colour charges	26
6.2	Ginzburg-Landau approach	27
6.3	Quark-hadron continuity and $U(1)_A$ anomaly	28
6.4	Collective excitations	30
7	Inhomogeneous states	31
7.1	Chiral-density waves	31
7.2	Implications from chromomagnetic instability	32
8	Suggestions from QCD-like theories	36
8.1	Quarkyonic matter at large N_c	36
8.2	QCD at $N_c = 2$	37
8.3	Ultracold atoms	38
9	Summary and concluding remarks	38

1. Introduction

One of the most crucial properties in the non-Abelian gauge theory of quarks and gluons, Quantum Chromodynamics (QCD) [1], is the asymptotic freedom [2, 3]; the coupling constant runs towards a smaller value with increasing energy scale. It is hence a natural anticipation that QCD matter at high energy densities undergoes a phase transition from a state with confined hadrons into a new state of matter with on-shell (real) quarks and gluons.

There are two important external parameters for QCD in equilibrium, the temperature T and the baryon number density n_B . (In the grand canonical ensemble,

the quark chemical potential $\mu_q = \mu_B/3$ may be introduced as a conjugate variable to the quark number density $n_q = 3n_B$.) Since the intrinsic scale of QCD is $\Lambda_{\text{QCD}} \sim 200 \text{ MeV}$, it would be conceivable that the QCD phase transition should take place around $T \sim \Lambda_{\text{QCD}} \sim \mathcal{O}(10^{12}) \text{ K}$ or $n_B \sim \Lambda_{\text{QCD}}^3 \sim 1 \text{ fm}^{-3}$. Experimentally, the heavy-ion collisions (HIC) in laboratories provide us with a chance to create hot and/or denser QCD matter and elucidate its properties. In particular, the Relativistic Heavy-Ion Collider (RHIC) at Brookhaven National Laboratory (BNL) has conducted experiments to create hot QCD matter (a quark-gluon plasma or QGP in short) by the Au-Au collisions with the highest collision energy $\sqrt{s_{NN}} = 200 \text{ GeV}$ [4]. The Large Hadron Collider (LHC) at CERN will continue experiments along the same line with higher energies [4, 5]. Exploration of a wider range of the QCD phase diagram with n_B up to several times of the normal nuclear matter density $n_0 \simeq 0.17 \text{ fm}^{-3}$ may be carried out by low-energy scan in HIC at RHIC as well as at the future facilities such as the Facility for Antiproton and Ion Research (FAIR) at GSI, the Nuclotron-based Ion Collider Facility (NICA) at JINR and the Japan Proton Accelerator Research Complex (J-PARC) at JAERI.

In nature, the deep interior of compact stellar objects such as neutron stars would be the relevant place where dense QCD matter at low temperature is realized (see [6] for a review). In fact, continuous efforts have been and are being conducted in the observations of neutron stars to extract information of the equation of state of dense QCD. If the baryon density is asymptotically high, weak coupling QCD analyses indicate that the QCD ground state forms a condensation of quark Cooper pairs, namely the colour superconductivity (CSC). Since quarks have not only spin but also colour and flavour quantum numbers, the quark pairing pattern is much more intricate than the electron pairing in metallic superconductors.

In this review we will discuss selected topical developments in the QCD phase diagram with an emphasis on the phases at finite μ_B . For the topics not covered in the present article, readers may consult other reviews [7, 8, 9, 10, 11, 12, 13, 14, 15, 16, 17, 18, 19].

We organize this article as follows. In section 2, after a brief introduction of two key features of hot/dense QCD, i.e. the deconfinement and chiral restoration, we show a conjectured QCD phase diagram in μ_B - T plane. In section 3 we introduce three major order parameters to characterize QCD matter at finite T and μ_B , i.e. the Polyakov loop, the chiral condensate and the diquark condensate. In section 4 we summarize the current status on the chiral phase transition at finite T with $\mu_B = 0$. In section 5 we go into more details about the phase transitions in the density region up to a moderate μ_B comparable to T , which are classified according to different spontaneous chiral symmetry breaking ($S\chi B$) patterns. We then address the situation with μ_B much greater than T in section 6. Even though the theoretical understanding has not been fully settled down yet, section 7 is devoted to a review over conjectured inhomogeneous states of QCD matter as well as some alternative scenarios. In section 8 we look over suggestive results and implications from QCD-like theories. Section 9 is devoted to the summary and concluding remarks.

2. QCD phase structure

We will run through the QCD phase transitions and associated phase structure here before detailed discussions in subsequent sections.

2.1. Deconfinement and chiral restoration

A first prototype of the QCD phase diagram in T - n_B plane was conjectured in [20]. It was elucidated that one could give an interpretation of the Hagedorn's limiting temperature in the Statistical Bootstrap Model (SBM) [21] as a critical temperature associated with a second-order phase transition into a new state of matter. The weakly interacting quark matter at large n_B due to the asymptotic freedom had been also recognized [22]. Historical summary of QCD phase diagram and its exploration in HIC experiments are given in the reviews [23, 24].

- *Deconfinement* — In an early picture of hadron resonance gas at finite temperature [25], the density of (mostly mesonic) states $\rho(m)$ as a function of the resonance mass m is proportional to $\exp(m/T^H)$ where $T^H \simeq 0.19$ GeV is known from the Regge slope parameter. Such an exponentially growing behaviour of the density of states should be balanced by the Boltzmann factor $\exp(-m/T)$ in the partition function. When $T > T^H$, the integration over m becomes singular, so that T^H plays a role of the limiting temperature (Hagedorn temperature) above which the hadronic description breaks down. This argument is applied to estimate the critical value of μ_B as well. The density of baryonic states, $\rho_B(m_B) \propto \exp(m_B/T_B^H)$, is balanced by the Boltzmann factor $\exp[-(m_B - \mu_B)/T]$, leading to the limiting temperature $T = (1 - \mu_B/m_B)T_B^H$. We see equivalently that the critical μ_B at $T = 0$ is given by $m_B (\gtrsim 1 \text{ GeV})$.

If one bears in mind a simple bag-model picture that hadrons are finite-size objects in which valence quarks are confined, it is conceivable to imagine that hadrons overlap with each other and start to percolate at the Hagedorn temperature [26, 27], which is an intuitive portrayal of quark deconfinement. Although the Hagedorn/percolation picture is useful for practical objectivization, it is necessary to develop a field-theoretical definition of the quark-deconfinement in QCD. Global centre symmetry of pure gluonic sector of QCD gives such a definition as elucidated in section 3.1.

- *Chiral restoration* — The QCD vacuum should be regarded as a medium with full of quantum fluctuations that are responsible for the generation of non-perturbative quark mass. In hot and dense energetic matter, quarks turn bare due to asymptotic freedom. Therefore, one may expect a phase transition from a state with heavy *constituent* quarks to another state with light *current* quarks. Such a transition is called chiral phase transition named after the underlying chiral symmetry of QCD. The QCD phase diagram at finite T and μ_B was also conjectured from the point of view of chiral symmetry [28]. In this case, the order parameter is the chiral condensate $\langle \bar{\psi}\psi \rangle$ which takes a value about $-(0.24 \text{ GeV})^3$ in the vacuum and sets a natural scale for the critical temperature of chiral restoration. In the chiral perturbation theory (χ Pt) the chiral condensate for two massless quark flavours at low temperature is known to behave as $\langle \bar{\psi}\psi \rangle_T / \langle \bar{\psi}\psi \rangle = 1 - T^2/(8f_\pi^2) - T^4/(384f_\pi^4) - \dots$ with the pion decay constant $f_\pi \simeq 93 \text{ MeV}$ [29]. Although the validity of χ Pt is limited to low temperature, this is a clear evidence of the melting of chiral condensate at finite temperature. At low baryon density, likewise, the chiral condensate decreases as $\langle \bar{\psi}\psi \rangle_{n_B} / \langle \bar{\psi}\psi \rangle = 1 - \sigma_{\pi N} n_B / (f_\pi^2 m_\pi^2) - \dots$ [30, 31, 32] where $\sigma_{\pi N} \sim 40 \text{ MeV}$ is the π - N sigma term. (For higher-order corrections, see [33, 34].)

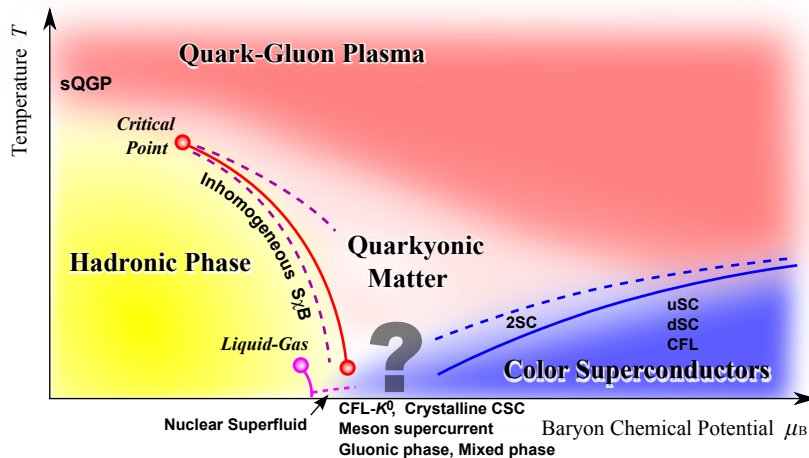


Figure 1. Conjectured QCD phase diagram with boundaries that define various states of QCD matter based on $S\chi B$ patterns.

The chiral transition is a notion independent of the deconfinement transition. In section 3.2 we classify the chiral transition according to the $S\chi B$ pattern.

2.2. Conjectured QCD phase diagram

Figure 1 summarizes our state-of-the-art understanding on the phase structure of QCD matter including conjectures which are not fully established. At present, relatively firm statements can be made only in limited cases – phase structure at finite T with small baryon density ($\mu_B \ll T$) and that at asymptotically high density ($\mu_B \gg \Lambda_{\text{QCD}}$). Below we will take a closer look at figure 1 from a smaller to larger value of μ_B in order.

Hadron-quark phase transition at $\mu_B = 0$: The QCD phase transition at finite temperature with zero chemical potential has been studied extensively in the numerical simulation on the lattice. Results depend on the number of colours and flavours as expected from the analysis of effective theories on the basis of the renormalization group together with the universality [35, 36]. A first-order deconfinement transition for $N_c = 3$ and $N_f = 0$ has been established from the finite size scaling analysis on the lattice [37], and the critical temperature is found to be $T_c \simeq 270$ MeV. For $N_f > 0$ light flavours it is appropriate to address more on the chiral phase transition. Recent analyses on the basis of the staggered fermion and Wilson fermion indicate a crossover from the hadronic phase to the quark-gluon plasma for realistic u , d and s quark masses [38, 39]. The pseudo-critical temperature T_{pc} , which characterizes the crossover location, is likely to be within the range 150 MeV – 200 MeV as summarized in section 4.2.

Even for the temperature above T_{pc} the system may be strongly correlated and show non-perturbative phenomena such as the existence of hadronic modes or pre-formed hadrons in the quark-gluon plasma at $\mu_B = 0$ [28, 40] as well as at $\mu_B \neq 0$ [41, 42, 43]. Similar phenomena can be seen in other strong coupling systems such as

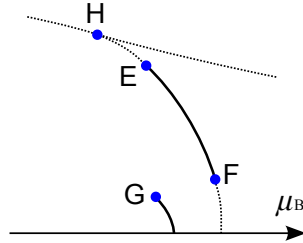


Figure 2. Characteristic points on the QCD phase diagram. E represents so-called the QCD critical point. F is another critical point induced by the quark-hadron continuity. G is the critical point associated with the liquid-gas transition of nuclear matter. H refers to a region which looks like an approximate triple point. See the text for details.

the high-temperature superconductivity and in the BEC regime of ultracold fermionic atoms [44].

QCD critical points: In the density region beyond $\mu_B \sim T$ there is no reliable information from the first-principle lattice QCD calculation. Investigation using effective models is a pragmatic alternative then. Most of the chiral models suggest that there is a *QCD critical point* located at $(\mu_B = \mu_E, T = T_E)$ and the chiral transition becomes first-order (crossover) for $\mu_B > \mu_E$ ($\mu_B < \mu_E$) for realistic u , d and s quark masses [45, 46, 47, 48] (see the point E in figure 2). The criticality implies enhanced fluctuations, so that the search for the QCD critical point is of great experimental interest [49, 50].

There is also a possibility that the first-order phase boundary ends at another critical point in the lower- T and higher- μ_B region whose location we shall denote by (μ_F, T_F) as shown by the point F in figure 2. As discussed in section 6, the cold dense QCD matter with three degenerate flavours may have no clear border between superfluid nuclear matter and superconducting quark matter, which is called the *quark-hadron continuity*.

In reality, the fate of the above critical points (E and F) depend strongly on the relative magnitude of the strange quark mass m_s and the typical values of T and μ_B at the phase boundary.

Liquid-gas phase transition of nuclear matter: Since the nucleon mass is $m_N \simeq 939$ MeV and the binding energy in isospin-symmetric nuclear matter is around 16 MeV, a non-vanishing baryon density of nuclear matter starts arising at $\mu_B = \mu_{\text{NM}} \simeq 924$ MeV at $T = 0$. At the threshold $\mu_B = \mu_{\text{NM}}$, the density n_B varies from zero to the normal nuclear density $n_0 = 0.17 \text{ fm}^{-3}$. For $0 < n_B < n_0$ the nuclear matter is fragmented into droplets with $n_B = n_0$, so that $n_B < n_0$ is achieved on spatial average. This is a typical first-order phase transition of the liquid-gas type. The first-order transition weakens as T grows and eventually ends up with a second-order critical point at (μ_G, T_G) as indicated by the point G in figure 2. Low energy HIC experiments indicate that $\mu_G \sim \mu_{\text{NM}}$ and $T_G = 15 \sim 20$ MeV [51].

Quaknyonic matter: The Statistical Model is successful to reproduce the experimentally observable particle abundances at various $\sqrt{s_{\text{NN}}}$ and thus various μ_B . This

model assumes a thermally equilibrated gas of non-interacting mesons, baryons and resonances for a given T and μ_B [52, 53, 54]. Within the model description one can extract T and μ_B from the HIC data by fitting the particle ratios. The accumulation of extracted points makes a curve on the μ_B - T plane, which is called the chemical freeze-out line.

The freeze-out line is not necessarily associated with any of QCD phase boundaries. Nevertheless, there is an argument to claim that the sudden freeze-out of chemical compositions should take place close to the phase transition [55]. Along the freeze-out line the thermal degrees of freedom are dominated by mesons for $\mu_B \ll m_N$. The higher μ_B becomes, the more baryons are excited. This indicates that there must be a transitional change at (T_H, μ_H) , where the importance of baryons in thermodynamics surpasses that of mesons. This happens around $\mu_H = 350 \sim 400$ MeV and $T_H = 150 \sim 160$ MeV according to the Statistical Model analysis.

It is interesting that such a phase structure is suggested from the large N_c limit of QCD. When N_c is large, quark loops are suppressed by $1/N_c$ as compared to gluon contributions [56, 57]. A finite baryon number density arises and the pressure grows of order N_c once μ_B becomes greater than the lowest baryon mass M_B . Such cold dense matter in the $N_c = \infty$ world is named *quarkyonic matter* [58]. Then, the phase diagram of large- N_c QCD consists of three regions separated by first-order phase transitions, i.e. the confined, deconfined and quarkyonic phases. The meeting point of the three first-order phase boundaries is the *triple point* whose remnant for finite N_c is indicated by the point H in figure 2, as suggested in [59]. We will revisit the idea of quarkyonic matter in section 8.1.

Colour superconductivity: If μ_B is asymptotically large, i.e. $\mu_B \gg \Lambda_{\text{QCD}}$, the ground state of QCD matter can be analyzed in terms of the weak-coupling methods in QCD. Also we can count on the knowledge from condensed matter physics with quarks substituting for electrons. In this analogue between electrons in metal and quarks in quark matter, one may well anticipate that the ground state of QCD matter at low T should form Cooper pairs leading to colour superconductivity (CSC) [13, 15, 18, 19, 60, 61]. Theoretical characterization will be further elucidated in section 3.3 and section 6.

There are many patterns of Cooper pairing and thus many different CSC states. The search for the most stable CSC state still remains unsettled except for $\mu_q \gg \Lambda_{\text{QCD}}$ or $m_s \rightarrow 0$. It is in fact the strange quark mass m_s that makes the problem cumbersome. In the intermediate density region particularly, the Fermi surface mismatch $\delta\mu_q$ of different quark flavours is given by $\delta\mu_q \sim m_s^2/\mu_q$. When the gap energy Δ is comparable with $\delta\mu_q$, an inhomogeneous diquark condensation may have a chance to develop energetically. Such an inhomogeneous CSC state gives rise to a crystal structure with respect to $\Delta(x)$, that is the crystalline CSC phase [62]. There are, at the same time, various candidates over the crystalline CSC phase in this intermediate density region and the true ground state has not been fully revealed there (see section 7).

So far we have quickly looked over the key phases labelled in figure 1 and important points specifically picked up in figure 2. In section 3 we will proceed to the theoretical framework to deal with the phase transitions of quark deconfinement and chiral restoration, respectively.

3. Order parameters for the QCD phase transition

QCD has (at least) three order parameters for quark deconfinement, chiral symmetry restoration and colour superconductivity as discussed below.

3.1. Polyakov loop and quark deconfinement

The Polyakov loop which characterizes the deconfinement transition in Euclidean space-time is defined as [63, 64]

$$L(\mathbf{x}) = \mathcal{P} \exp \left[-ig \int_0^\beta dx_4 A_4(\mathbf{x}, x_4) \right], \quad (1)$$

which is an $N_c \times N_c$ matrix in colour space. Here β is the inverse temperature $\beta = 1/T$, and \mathcal{P} represents the path ordering. We will use ℓ to represent the traced Polyakov loop,

$$\ell = \frac{1}{N_c} \text{tr} L. \quad (2)$$

Let us consider the centre $Z(N_c)$ of the colour gauge group $SU(N_c)$: elements of the centre commute with all $SU(N_c)$ elements and can be written as $z_k \mathbb{1}$ with $z_k = e^{2\pi i k/N_c}$ ($k = 0, 1, \dots, N_c - 1$) and $\mathbb{1}$ being an $N_c \times N_c$ unit matrix. Under a non-periodic gauge transformation of the following form; $V_k(x) = [z_k \mathbb{1}]^{x_4/\beta}$, the gauge fields receive a constant shift,

$$A_4 \longrightarrow A_4^k = V_k [A_4 - (ig)^{-1} \partial_4] V_k^\dagger = A_4 - \frac{2\pi k}{g N_c \beta}, \quad (3)$$

so that the traced Polyakov loop transforms as $\ell \rightarrow z_k \ell$. Because A_4^k still keeps the periodicity in x_4 , such a non-periodic gauge transformation still forms a symmetry of the gauge action. This is called centre symmetry [8, 35]. The quark action (with the quark field denoted by ψ) explicitly breaks centre symmetry because the transformed field $V_k(x)\psi(x)$ does not respect the anti-periodic boundary condition any longer. Thus, centre symmetry is an exact symmetry only in the pure gluonic theory where dynamical quarks are absent or quark masses are infinitely heavy ($m_q \rightarrow \infty$).

The expectation value of the Polyakov loop and its correlation in the pure gluonic theory can be written as [65, 66, 67]

$$\Phi = \langle \ell(\mathbf{x}) \rangle = e^{-\beta f_q}, \quad \bar{\Phi} = \langle \ell^\dagger(\mathbf{x}) \rangle = e^{-\beta f_{\bar{q}}}, \quad (4)$$

$$\langle \ell^\dagger(\mathbf{x}) \ell(\mathbf{y}) \rangle = e^{-\beta f_{q\bar{q}}(\mathbf{x}-\mathbf{y})}. \quad (5)$$

Here, the constant f_q ($f_{\bar{q}}$) independent of \mathbf{x} is an excess free energy for a static quark (anti-quark) in a hot gluon medium. [‡] Also, $f_{q\bar{q}}(\mathbf{x}-\mathbf{y})$ is an excess free energy for an anti-quark at \mathbf{x} and a quark at \mathbf{y} . [§]

In the confining phase of the pure gluonic theory, the free energy of a single quark diverges ($f_q \rightarrow \infty$) and the potential between a quark and an anti-quark increases linearly at long distance ($f_{q\bar{q}}(r \rightarrow \infty) \rightarrow \sigma r$ with $r = |\mathbf{x} - \mathbf{y}|$), which leads to $\Phi \rightarrow 0$ and $\langle \ell^\dagger(r \rightarrow \infty) \ell(0) \rangle \rightarrow 0$. On the other hand, in the deconfined phase, the free

[‡] Strictly speaking, the expectation value in the pure gluonic theory $\langle \ell(\mathbf{x}) \rangle$ should be defined by taking the limit $m_q \rightarrow +\infty$ after taking the thermodynamic limit $V \rightarrow \infty$, so that it takes a real value. Alternatively, one may use $|\langle \ell(\mathbf{x}) \rangle|$ to define the free energy of a single quark.

[§] Even when there are dynamical quarks, one may use the Polyakov loops, (4) and (5), to define the heavy-quark free energies.

	Confined (Disordered) Phase	Deconfined (Ordered) Phase
Free Energy	$f_q = \infty$	$f_q < \infty$
	$f_{\bar{q}q} \sim \sigma r$	$f_{\bar{q}q} \sim f_q + f_{\bar{q}} + \alpha \frac{e^{-m_M r}}{r}$
Polyakov Loop	$\langle \ell \rangle = 0$	$\langle \ell \rangle \neq 0$
$(r \rightarrow \infty)$	$\langle \ell^\dagger(r)\ell(0) \rangle \rightarrow 0$	$\langle \ell^\dagger(r)\ell(0) \rangle \rightarrow \langle \ell \rangle ^2 \neq 0$

Table 1. Behaviour of the expectation value and the correlation of the Polyakov loop in the confined and deconfined phases in the pure gluonic theory.

energy of a single quark is finite ($f_q < \infty$). Also the potential between a quark and an anti-quark is of the Yukawa type at long distance with a magnetic screening mass m_M [68, 69, 70],

$$f_{\bar{q}q}(r \rightarrow \infty) \rightarrow f_{\bar{q}} + f_q + \alpha \frac{e^{-m_M r}}{r}, \quad (6)$$

where α is a dimensionless constant. Note that the glueball exchange with mass of $O(g^2 T)$ which is smaller than the electric screening scale $O(gT)$ dominates over the long-range correlation at weak coupling. Therefore, $\Phi \neq 0$ and $\langle \ell^\dagger(r \rightarrow \infty)\ell(0) \rangle \neq 0$.

The qualitative behaviour of $\Phi = \langle \ell \rangle$ and $\langle \ell^\dagger \ell \rangle$ is summarized in table 1. We see that Φ can nicely characterize the state of matter in such a way that ℓ behaves like a magnetization in 3D classical spin systems [35, 8, 71]. The pure gluonic theory for $N_c = 2$ and 3 have been studied in lattice gauge simulations with the finite-size scaling analysis [72, 37]. It was shown that there is a second-order phase transition for $N_c = 2$ and a first-order phase transition for $N_c = 3$: For $N_c = 2$ the critical exponent is found to agree with the Z(2) Ising model in accordance with the universality. For $N_c = 3$ the Ginzburg-Landau free energy for the Polyakov loop has a cubic invariant, so that the first-order transition can naturally be induced [8, 37, 73]. Recent studies of the pure gluonic theory with $N_c = 4, 6, 8, 10$ indicate that the transition is of first order for $N_c \geq 3$ and becomes stronger as N_c increases [74, 75]. This behavior is similar to that of the 3D N_c -state Potts model [76].

The idea to construct the deconfinement order parameter can be extended to a more general setup. Suppose that there is an arbitrary operator \mathcal{O} written in terms of gauge fields that is not invariant under centre transformation. (If we take \mathcal{O} as the quark propagator straight up along the imaginary-time direction, the following argument shall result in the standard definition of the Polyakov loop.) The expectation value of \mathcal{O} in the pure gluonic theory can be decomposed by the triality projection [77]; $\langle \mathcal{O}[A] \rangle_{\text{pure}} = \sum_{n=0}^{N_c-1} \langle \mathcal{O}_n[A] \rangle_{\text{pure}}$ with

$$\langle \mathcal{O}_n[A] \rangle_{\text{pure}} = \frac{1}{N_c} \sum_{k=0}^{N_c-1} \langle \mathcal{O}[A^k] \rangle_{\text{pure}} e^{-2\pi i k n / N_c}, \quad (7)$$

where A^k is defined in (3). Then, $\langle \mathcal{O}_n[A] \rangle_{\text{pure}}$ with $n \neq 0$ can be an order parameter sensitive to the spontaneous breaking of centre symmetry. A particular choice $\mathcal{O} = \bar{\psi}\psi$ [78, 79] (so-called the dual condensate) has some practical advantages [80].

Centre symmetry discussed so far is rigorously defined only in the pure gluonic system as already mentioned: In the presence of dynamical quarks, centre symmetry is broken explicitly, so that Φ and $\bar{\Phi}$ always take finite values. This is analogous to the spin system under external magnetic field, in which the magnetization is always non-vanishing [81]. Nevertheless, Φ may be estimated as $\Phi = e^{-\beta M}$ with a hadronic

mass scale ($M \sim 0.8 \text{ GeV}$) at low T and thus the low- T phase approximately preserves centre symmetry.

3.2. Chiral condensate and dynamical breaking of chiral symmetry

In the QCD vacuum at $T = \mu_B = 0$, chiral symmetry is spontaneously broken, which is the source of hadron masses. It is a common wisdom that the chiral symmetry breaking is driven by the expectation value of an operator which transforms as $(N_f, N_f^*) + (N_f^*, N_f)$ under chiral symmetry. A simplest choice of the order parameter for the chiral symmetry breaking is a bilinear form called the chiral condensate,

$$\langle \bar{\psi}\psi \rangle = \langle \bar{\psi}_R \psi_L + \bar{\psi}_L \psi_R \rangle, \quad (8)$$

where colour and flavour indices of the quark fields are to be summed. If the above chiral condensate is non-vanishing even after taking the limit of zero quark masses, chiral symmetry is spontaneously broken according to the pattern $\mathcal{G} \rightarrow \mathcal{H}$ with

$$\mathcal{G} = \text{SU}(N_f)_L \times \text{SU}(N_f)_R \times \text{U}(1)_B \times \text{Z}(2N_f)_A \quad (9)$$

$$\mathcal{H} = \text{SU}(N_f)_V \times \text{U}(1)_B, \quad (10)$$

which leads to $N_f^2 - 1$ massless Nambu-Goldstone bosons for $N_f > 1$. \parallel The $\text{U}(1)_A$ symmetry in the classical level of the QCD Lagrangian is broken down explicitly to $\text{Z}(2N_f)_A$ in the quantum level. Then, the $\text{U}(1)_A$ current is no longer conserved ($\text{U}(1)_A$ anomaly); \blacktriangleleft

$$\partial_\mu j_5^\mu = -\frac{g^2 N_f}{32\pi^2} \epsilon^{\alpha\beta\mu\nu} F_{\alpha\beta}^a F_{\mu\nu}^a. \quad (11)$$

The right-hand side of the above relation is nothing but the topological charge density. Thus, gauge configurations with non-trivial topology are microscopically responsible for the $\text{U}(1)_A$ anomaly. In other words, the $\text{U}(1)_A$ current could be approximately conserved if the gauge configurations are dominated by topologically trivial sectors. We will come back to this point later to address *effective* restoration of $\text{U}(1)_A$ symmetry in the medium [83].

Note that (8) is not a unique choice for the order parameter [84, 85, 86, 87]. For example, one may consider the following four-quark condensate,

$$\left\langle \bar{\psi} \frac{\lambda^a}{2} (1 - \gamma_5) \psi \cdot \bar{\psi} \frac{\lambda^a}{2} (1 + \gamma_5) \psi \right\rangle = \left\langle \bar{\psi}_R \lambda^a \psi_L \cdot \bar{\psi}_L \lambda^a \psi_R \right\rangle. \quad (12)$$

If this is non-vanishing, the ground state breaks chiral symmetry \mathcal{G} to $\mathcal{H} \times \text{Z}(N_f)_A$ where $\text{Z}(N_f)_A$ corresponds to a discrete axial rotation. If the bilinear condensate (8) is non-zero, the four-quark condensate (12) takes a finite value in general. However, a non-zero value of (12) does not necessarily enforce a finite value of (8). In fact, if $\text{Z}(N_f)_A$ symmetry is left unbroken, (8) must vanish. As long as the Dirac determinant in QCD is positive definite, possibility of unbroken $\text{Z}(N_f)_A$ symmetry has been ruled out by the exact QCD inequality [85]. However, it is not necessary the case for finite μ_B with which the positivity of the Dirac determinant does not hold.

\parallel Strictly speaking, the quotient groups $\mathcal{G}' = \mathcal{G}/[\text{Z}(N_f) \times \text{Z}(N_f)]$ and $\mathcal{H}' = \mathcal{H}/\text{Z}(N_f)$ need to be introduced to avoid double counting of the discrete centre group operation. A simplest example of this kind is $\text{U}(N) = [\text{SU}(N) \times \text{U}(1)]/\text{Z}(N)$ [82].

\blacktriangleleft The anomaly relation does not necessarily guarantee the absence of the massless Nambu-Goldstone boson. In the Schwinger model which is an exactly solvable QCD analogue, the $\text{U}(1)_A$ problem is resolved by the Kogut-Susskind dipole ghosts.

3.3. Diquark condensate and colour superconductivity

QCD at high baryon density shows a novel mechanism of spontaneous chiral symmetry breaking [88]. The fundamental degrees of freedom in the CSC phase with three colours and three flavours are the diquarks defined as

$$(\varphi_L^\dagger)_{\alpha i} \sim \epsilon_{\alpha\beta\gamma} \epsilon_{ijk} (\psi_L^\dagger)_{\beta j} C(\psi_L)_{\gamma k}, \quad (\varphi_R^\dagger)_{\alpha i} \sim \epsilon_{\alpha\beta\gamma} \epsilon_{ijk} (\psi_R^\dagger)_{\beta j} C(\psi_R)_{\gamma k}, \quad (13)$$

where (i, j, k) are flavour indices and (α, β, γ) are colour indices. Note that the charge conjugation matrix $C = i\gamma^2\gamma^0$ is necessary to make $\varphi_{L/R}$ be Lorentz scalar. Then, $\varphi_{L/R}$ is a triplet both in colour and flavour, so that it transforms in the same way as the quark field $\psi_{L/R}$.

Under certain gauge fixing, one may consider the expectation values of these operators. They are called the diquark condensates as will be discussed further in section 6. Instead, we can also construct an analogue of (8) in terms of the diquarks,

$$\langle \varphi_R^\dagger \varphi_L \rangle + \langle \varphi_L^\dagger \varphi_R \rangle, \quad (14)$$

where colour and flavour indices are summed. This is a gauge-invariant four-quark condensate which characterizes the spontaneous chiral symmetry breaking in CSC [13]. Unlike the bilinear operator in (8), the four-quark operator here keeps additional invariance $Z(2)_L \times Z(2)_R$ corresponding to the reflections; $\psi_L \rightarrow -\psi_L$ and $\psi_R \rightarrow -\psi_R$, which is broken down to $Z(2)$ due to the $U(1)_A$ anomaly.

In the CSC phase, not only chiral symmetry but also $U(1)_B$ symmetry associated with the baryon number conservation may be spontaneously broken. A colour singlet order parameter to detect such symmetry breaking can be

$$\epsilon_{\alpha\beta\gamma} \epsilon_{ijk} \langle (\varphi_{L/R})_{\alpha i} (\varphi_{L/R})_{\beta j} (\varphi_{L/R})_{\gamma k} \rangle. \quad (15)$$

The six-quark operator here breaks $U(1)_B$ with its $Z(6)_B$ subgroup maintained. If this condensate is non-zero, there appears exactly massless Nambu-Goldstone boson because the baryon number symmetry is an exact symmetry in the QCD Lagrangian.

4. Chiral phase transition at finite temperature

The chiral phase transition at finite T with $\mu_B = 0$ has been and is being extensively studied by the renormalization group method near the critical point à la Ginzburg-Landau-Wilson and by the lattice-QCD simulations. In this section we will briefly summarize the current status of these studies. (See [39] for further details.)

4.1. Ginzburg-Landau-Wilson analysis

If the phase transition is of second order or of weak first order, one may write down the free-energy functional in terms of the order parameter field Φ as a power series of Φ/T_c . The large fluctuation of Φ near the critical point is then taken into account by the renormalization group method. This is called the Ginzburg-Landau-Wilson approach. For chiral phase transition in QCD, the relevant order parameter field is a $N_f \times N_f$ matrix in flavour space, $\Phi_{ij} \sim \langle \bar{\psi}_j(1 - \gamma_5)\psi_i \rangle$. Under the flavour chiral rotation $U(N_f)_L \times U(N_f)_R$, Φ transforms as $\Phi \rightarrow V_L \Phi V_R^\dagger$. Then the Ginzburg-Landau free energy in three spatial dimensions ($D = 3$) with full $U(N_f)_L \times U(N_f)_R$ symmetry up to the quartic order in Φ_{ij} becomes [36, 47];

$$\Omega_{\text{sym}} = \frac{1}{2} \text{tr} \nabla \Phi^\dagger \nabla \Phi + \frac{a_0}{2} \text{tr} \Phi^\dagger \Phi + \frac{b_1}{4!} (\text{tr} \Phi^\dagger \Phi)^2 + \frac{b_2}{4!} \text{tr} (\Phi^\dagger \Phi)^2. \quad (16)$$

	$N_f = 2$	$N_f \geq 3$
$U(1)_A$ symmetric ($c_0 = 0$)	Fluctuation-induced 1st order	1st order
$U(1)_A$ broken ($c_0 \neq 0$)	2nd order [O(4) universality]	1st order

Table 2. Order of the chiral phase transition conjectured from the chiral effective theory with massless N_f flavours with and without the $U(1)_A$ anomaly.

Effects of temperature T enter through the parameters a_0 , b_1 and b_2 . Note that Ω_{sym} is bounded from below as long as $b_1 + b_2/N_f > 0$ and $b_2 > 0$ are satisfied. The renormalization group analysis of (16) on the basis of the leading-order $\epsilon (= 4 - D)$ expansion leads to a conclusion that there is no stable IR fixed point for $N_f > \sqrt{3}$ [36]. This implies that the thermal phase transition described by (16) is of the fluctuation-induced first order for two or more flavours.

In QCD, however, there is $U(1)_A$ anomaly and the correct chiral symmetry is $SU(N_f)_L \times SU(N_f)_R \times U(1)_B \times Z(2N_f)_A$ for N_f massless quarks. The lowest dimensional operator which breaks $U(1)_A$ symmetry explicitly while keeping the rest of chiral symmetry is the Kobayashi–Maskawa–’t Hooft (KMT) term [89, 90, 91, 92];

$$\Omega_{\text{anomaly}} = -\frac{c_0}{2} (\det \Phi + \det \Phi^\dagger). \quad (17)$$

The coefficient c_0 , which is T -dependent in general, dictates the strength of $U(1)_A$ anomaly. In the instanton picture [91, 92], $c_0(T = 0)$ is proportional to the instanton density n_{inst} , which is perturbatively evaluated as [7]

$$c_0(T = 0) \propto n_{\text{inst}}(\rho, T = 0) = \left(\frac{8\pi^2}{g^2}\right)^{2N_c} e^{-8\pi^2/g^2} \rho^{-5}, \quad (18)$$

with ρ being a typical instanton size.

For $N_f = 3$ the KMT term becomes a cubic invariant in the order parameter. Hence, $\Omega[\Phi] = \Omega_{\text{sym}} + \Omega_{\text{anomaly}}$ leads to the chiral phase transition of first order. For $N_f = 2$, on the other hand, the KMT term becomes a quadratic invariant. Also the chiral symmetry in this case is $SU(2)_L \times SU(2)_R \cong SO(4)$. Such an effective theory with O(4) symmetry has a Wilson-Fisher type IR fixed point as long as the coefficient of the quartic term of Φ is positive. Therefore, *if* the chiral phase transition of massless $N_f = 2$ QCD is of second order, its critical exponents would be the same as those in the 3D O(4) effective theory according to the notion of universality. In Table 2 we summarize the Ginzburg-Landau-Wilson analysis from the chiral effective theory [36].

In the real world, none of quark is exactly massless: For example, $m_u = (1.5\text{--}3.3)\text{ MeV}$, $m_d = (3.5\text{--}6.0)\text{ MeV}$ and $m_s = 105_{-35}^{+25}\text{ MeV}$ at the renormalization scale of 2 GeV [93]. Therefore, it is useful to draw a phase diagram by treating quark masses as external parameters. This is called the Columbia plot [94] as shown in figure 3 where the isospin degeneracy is assumed ($m_u = m_d \equiv m_{\text{ud}}$). The first-order chiral transition and the first-order deconfinement transition at finite T are indicated by the left-bottom region and the right-top region, respectively. The chiral and deconfinement critical lines, which separate the first-order and crossover regions, belong to a universality class of the 3D Z(2) Ising model except for special points at $m_{\text{ud}} = 0$ or $m_s = 0$ [95].

If the chiral transition is of second order for massless $N_f = 2$ case, the Z(2) chiral critical line meets the $m_{\text{ud}} = 0$ axis at $m_s = m_s^{\text{tri}}$ (*tricritical point*) and changes its universality to O(4) for $m_s > m_s^{\text{tri}}$ [96]. The tricritical point at $m_s = m_s^{\text{tri}}$ is a Gaussian fixed point of the 3D ϕ^6 model (that is, the critical dimension is not 4 but 3 at the

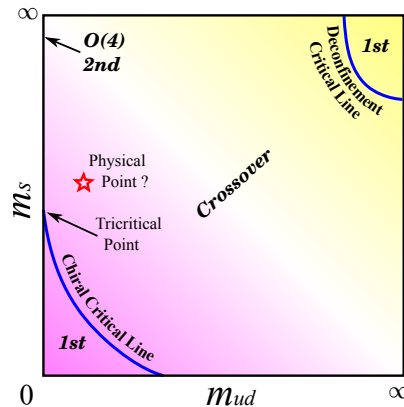


Figure 3. Schematic figure of the Columbia phase diagram in 3-flavour QCD at $\mu_B = 0$ on the plane with the light and heavy quark masses. The $U(1)_A$ symmetry restoration is not taken into account. Near the left-bottom corner the chiral phase transition is of first order and turns to smooth crossover as m_{ud} and/or m_s increase. The right-top corner indicates the deconfinement phase transition in the pure gluonic dynamics.

tricritical point), so that the critical exponents take the classical (mean-field) values [97], which is confirmed in numerical studies of the chiral model [98].

4.2. Lattice QCD simulations

Although the critical properties expected from the Ginzburg-Landau-Wilson analysis discussed above are expected to be universal, the quantities such as the critical temperature and the equation of state depend on the details of microscopic dynamics. In QCD, only a reliable method known for microscopic calculation is the lattice-QCD simulation in which the functional integration is carried out on the space-time lattice with a lattice spacing a and the lattice volume V by the method of importance sampling. In lattice-QCD simulations there are at least two extrapolations required to obtain physical results; the extrapolation to the continuum limit ($a \rightarrow 0$) and the extrapolation to the thermodynamic limit ($V \rightarrow \infty$). Therefore, lattice results receive not only statistical errors due to the importance sampling but systematic errors due to the extrapolations also.

For nearly massless fermions in QCD, there is an extra complication to reconcile chiral symmetry and lattice discretization; the Wilson fermion and the staggered fermion have been the standard ways to define light quarks on the lattice, while the domain-wall fermion and the overlap fermion recently proposed have more solid theoretical ground although the simulation costs are higher. For various applications of lattice-QCD simulations to the system at finite T and μ_B , see a recent review [39].

Here we mention only two points relevant to the discussions below: (i) The thermal transition for physical quark masses is likely to be crossover as indicated by a star-symbol in figure 3. This is based on the finite-size scaling analysis using staggered fermion [38]. Confirmation of this result by other fermion formalisms is necessary, however. (ii) The (pseudo)-critical temperature T_{pc} with different types of fermions and with different lattice spacings are summarized in figure 4. In view of these data with error bars, we adopt a conservative estimate at present; $T_{pc} = 150$ –

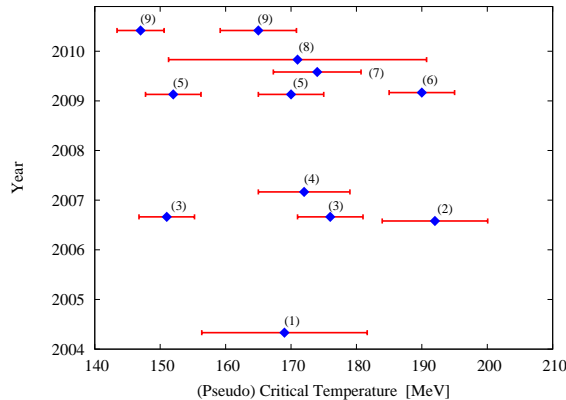


Figure 4. Determination of the pseudo-critical temperature T_{pc} for thermal QCD transition(s) from recent lattice QCD simulations. (1) 169(12)(4) MeV for 2 + 1 flavours in the asqtad action with N_t up to 8 determined by χ_m/T^2 (where χ_m is the chiral susceptibility) [99]. (2) 192(7)(4) MeV for 2 + 1 flavours in the p4fat3 staggered action with N_t up to 6 determined by χ_m and χ_L (where χ_L is the Polyakov loop susceptibility) [100]. (3) 151(3)(3) MeV and 176(3)(4) MeV for 2 + 1 flavours in the stout-link improved staggered action with N_t up to 10 determined by χ_m/T^4 and χ_L respectively [101]. (4) 172(7) MeV for 2 flavours in clover improved Wilson action with N_t up to 6 determined by χ_L [102]. (5) 152(3)(3) MeV and 170(4)(3) MeV for 2 + 1 flavours in the stout-link improved staggered action with N_t up to 12 determined by χ_m/T^2 and χ_L respectively [103]. (6) 185–195 MeV for 2 + 1 flavours in the asqtad and p4 actions with N_t up to 8 determined by χ_m and χ_L [104]. (7) 174(3)(6) MeV for 2 flavours in the improved Wilson action with N_t up to 12 determined by χ_m and χ_L [105]. (8) 171(10)(17) MeV for 2 + 1 flavours in the domain-wall action with $N_t = 8$ determined by χ_m/T^2 [106]. (9) 147(2)(3) MeV and 165(5)(3) MeV for 2 + 1 flavours in the stout-link improved staggered action with N_t up to 16 determined by χ_m/T^4 and χ_s/T^2 (where χ_s is the strange-quark susceptibility) [107].

200 MeV. ⁺ It has been clarified recently that improvement of the staggered action with less taste-symmetry breaking favours smaller value of $T_{\text{pc}} \lesssim 170$ MeV [107, 108].

5. Chiral phase transition at finite baryon density

Let us now introduce the baryon chemical potential μ_B as an extra axis to the Columbia plot. In the so-called “standard scenario” the first-order region in the lower left corner of the Columbia plot is elongated with increasing μ_B as written in the left panel of figure 5. If the physical point at $\mu_B = 0$ is in the crossover region, there arises a critical chemical potential μ_E so that the system shows a first-order transition for $\mu_B > \mu_E$. That is, we find a QCD critical point at (μ_E, T_E) on the QCD phase diagram in the μ_B - T plane. In the right of figure 5, the so-called “exotic scenario” is sketched, in which the size of the first-order region shrinks as μ_B increases. In this case, if the physical point at $\mu_B = 0$ is in the crossover region, it stays crossover for

⁺ Possible uncertainties in T_{pc} stem from discretization errors, conversion from the lattice unit to the physical unit, and the prescription of defining T_{pc} . For crossover transition T_{pc} may depend on which susceptibility (either chiral susceptibility $\chi_m(T)$ or Polyakov loop susceptibility $\chi_L(T)$) are used, and also depend on T -dependent normalization of the susceptibilities.

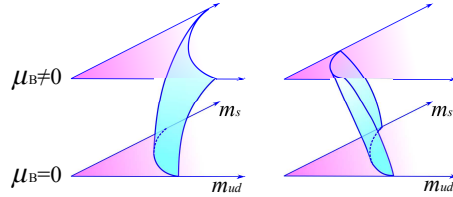


Figure 5. Schematic evolution of the Columbia plot with increasing μ_B in the standard scenario (left) and the exotic scenario (right).

finite μ_B , so that there arises no critical point (at least for small μ_B) in the QCD phase diagram in the μ_B - T plane. In general the critical surface in figure 5 can have more complicated structure, which may allow for several QCD critical points in the μ_B - T plane.

5.1. Lattice QCD at low baryon density

In the presence of $\mu_q \neq 0$, the QCD partition function on the lattice is written as

$$Z(T, \mu) = \int [dU] \det[F(\mu_q)] \exp^{-\beta S_{\text{YM}}(U)}, \quad (19)$$

where U is the matrix-valued gauge field defined on the links. The Yang-Mills action is denoted by $\beta S_{\text{YM}}(U)$ with $\beta = 2N_c/g^2$, while the quark contribution is denoted by the determinant of $F(\mu_q) = D(\mu_q) + m_q$ with $D(\mu_q)$ being the Euclidean Dirac operator. The quark mass m_q is real and positive. Let ψ be an eigenfunction of $D(\mu_q)$ as $D(\mu_q)\psi_i = \lambda_i\psi_i$ with an eigenvalue λ_i . If $\mu_q = 0$ then $D(0)$ is an anti-Hermitian operator and thus λ_i should be pure imaginary. Besides, $\gamma^5\psi_i$ is an independent eigenfunction with an eigenvalue $-\lambda_i = \lambda_i^*$, because of γ^5 -Hermiticity $\gamma^5 D(0)\gamma^5 = -D(0) = D^\dagger(0)$. Thus, we always have complex-conjugate pairs (λ_i, λ_i^*) and the determinant becomes real and positive;

$$\det[D(0) + m_q] = \prod_i (\lambda_i + m_q)(\lambda_i^* + m_q) > 0. \quad (20)$$

In this way, at $\mu_q = 0$, the integrand in (19) is positive definite and the importance sampling method works fine to evaluate the functional integral.

For $\mu_q \neq 0$ the γ^5 -Hermiticity is replaced by

$$\gamma^5 D(\mu_q)\gamma^5 = D^\dagger(-\mu_q^*). \quad (21)$$

Therefore $\det[D(\mu_q) + m_q]$ is no longer real unless μ_q is pure imaginary. This requires us to deal with a severe cancellation of positive and negative numbers to evaluate the functional integral. This is the notorious *sign problem* whose difficulty grows exponentially as the lattice volume V increases.

In the following we shall briefly look over some of approaches in the lattice-QCD simulations at finite μ_q . For more details, see the reviews [109, 110, 111] and references therein.

- *Multi-parameter reweighting method* — An expectation value of an operator \mathcal{O} at finite μ_q can be formally rewritten in terms of an ensemble average at $\mu_q = 0$;

$$\langle \mathcal{O} \rangle_{\mu_q} = \langle \mathcal{O} \cdot R(\mu_q) \rangle_{\mu_q=0} \langle R(\mu_q) \rangle_{\mu_q=0}^{-1}, \quad (22)$$

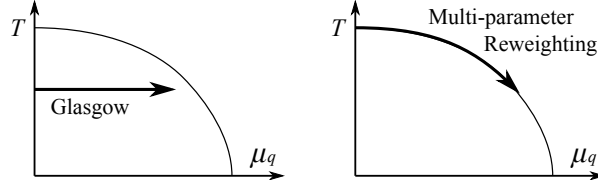


Figure 6. Conceptual illustration of the single-parameter reweighting method (Glasgow method) in the μ_q direction only and the multi-parameter reweighting method in the both μ_q and β (i.e. T) directions

where $R(\mu_q) \equiv \det F(\mu_q)/\det F(0)$ is called the reweighting factor [112]. The gauge configurations generated at $\mu_q = 0$ only occasionally sample the region where $\mathcal{O} \cdot R(\mu_q)$ and $R(\mu_q)$ are large (overlap problem). Also, they take complex values (sign problem). Therefore, such a simulation works only when μ_q and V are small.

To have a better overlap, the reweighting may be generalized towards not only the μ_q direction but also the β direction [113]:

$$\langle \mathcal{O} \rangle_{\mu_q} = \langle \mathcal{O} \cdot R(\mu_q, \delta\beta) \rangle_{\beta_0, \mu_q=0} \langle R(\mu_q, \delta\beta) \rangle_{\beta_0, \mu_q=0}^{-1}, \quad (23)$$

where the multi-parameter reweighting factor is defined as $R(\mu_q, \delta\beta) \equiv R(\mu_q) \exp(-\delta\beta S)$ with $\delta\beta = \beta - \beta_0$. Here β_0 should be chosen to maximize the overlap. The physical temperature T and $\beta = 2N_c/g^2$ are implicitly related through the lattice spacing a . Then, the reweighting along the phase boundary in the μ_q - $T(\beta)$ plane (as sketched in the right panel of figure 6) would have a better chance to probe into larger μ_q .

- *Taylor expansion method* — The full evaluation of the reweighting factor $R(\mu_q)$ is not an easy task even on the computer. If μ_q is small enough, the right-hand side of (22) can be expanded in terms of μ_q/T [114, 115, 116],

$$\begin{aligned} \langle \mathcal{O} \rangle_{\mu_q} &= \sum_{n=0}^{\infty} c_n \left(\frac{\mu_q}{T} \right)^n, \\ c_n &= \frac{T^n}{n!} \frac{\partial^n}{\partial \mu_q^n} \left(\langle \mathcal{O} \cdot R(\mu_q) \rangle_{\mu_q=0} \langle R(\mu_q) \rangle_{\mu_q=0}^{-1} \right). \end{aligned} \quad (24)$$

The coefficients c_n are written in terms of the quark propagator and can be simulated at $\mu_q = 0$. Because the expansion is based on (22), the original overlap problem translates into the convergence problem in higher order terms; the Taylor expansion makes sense for μ_q/T within a radius of convergence dictated by the singularity closest to the origin in the complex μ_q/T -plane.

- *Imaginary chemical potential method* — If μ_q is pure imaginary (which is here denoted by $\tilde{\mu}_q$), (21) reduces to the γ^5 -Hermiticity, so that there is no sign problem [117, 118]. Then, it is possible to perform lattice simulations to find physical observables by the analytic continuation back to the real chemical potential,

$$\langle \mathcal{O} \rangle_{\tilde{\mu}_q} = \sum_{n=0}^{\infty} c_n \left(\frac{\tilde{\mu}_q}{\mu_0} \right)^n \rightarrow \langle \mathcal{O} \rangle_{\mu_q} = \sum_{n=0}^{\infty} c_n \left(\frac{-i\mu_q}{\mu_0} \right)^n. \quad (25)$$

The applicability of this method is bounded by singularities or periodicity. For imaginary chemical potential, $\tilde{\mu}_q/T$ plays a role of an angle variable which has naïve periodicity by 2π . However, the partition function is a function of $\tilde{\mu}_q + gA_4$ and a change in $\tilde{\mu}_q$ by $2\pi/N_c$ can be absorbed by the centre transformation (3). Therefore, the actual period of $\tilde{\mu}_q/T$ is $2\pi/N_c$ (Roberge-Weiss (RW) periodicity) [119]. In the deconfinement phase at high T , especially, there is a first-order phase transition at a half of the RW point; $\tilde{\mu}_q/T = \pi/N_c \sim 1$ for $N_c = 3$. Thus the method of imaginary chemical potential works up to $\tilde{\mu}_q/T \lesssim 1$ at best, which is also confirmed in model studies [120].

- *Canonical ensemble method* — In the thermodynamic limit the canonical ensemble with fixed particle number N_q is equivalent with the grand canonical ensemble with fixed chemical potential μ_q (and the mean value of N_q is specified). To convert the grand canonical to the canonical description, the Fourier transform in terms of the imaginary chemical potential is necessary [121, 122, 123, 117, 124, 125],

$$\langle \mathcal{O} \rangle_{N_q} = \int_0^{2\pi} \frac{d\phi}{2\pi} e^{-iN_q\phi} \langle \mathcal{O} \rangle_{\tilde{\mu}_q = \phi T}. \quad (26)$$

In this case, the difficulty of the sign problem is transferred to the integration with respect to $\phi = \tilde{\mu}_q/T$. This canonical approach works fine as long as the volume is not large, for which centre symmetry is forced to be restored for N_q that is a multiple of N_c [77]. It is a highly delicate procedure to take the correct thermodynamic limit $V \rightarrow \infty$ in which not N_q but $n_q = N_q/V$ should be kept fixed. Especially, the order of the phase transition is sensitive to how the thermodynamic limit is approached [126].

- *Density of states method* — There are several variants of the density of states method depending on the choice of a variable to rewrite the partition function. Here we take an example of a phase θ of the Dirac determinant [127, 128]. (The plaquette P or energy E is useful as well [129, 130, 131].) The density of states in this case reads

$$\rho(\theta) = \langle \delta(\theta - \theta(U)) \rangle_{\text{pq}}, \quad (27)$$

where the expectation value is taken by the phase quenched simulation in which $\det F(\mu_q)$ is replaced by $|\det F(\mu_q)|$ to avoid the sign problem. Using $\rho(\theta)$ one can express the expectation value of an operator \mathcal{O} as

$$\langle \mathcal{O} \rangle_{\mu_q} = \frac{1}{Z} \int d\theta \rho(\theta) e^{i\theta} \langle \mathcal{O} \rangle_{\theta}, \quad (28)$$

with $Z = \int d\theta \rho(\theta) e^{i\theta}$ and

$$\langle \mathcal{O} \rangle_{\theta} = \frac{1}{\rho(\theta)} \langle \mathcal{O} \cdot \delta(\theta - \theta(U)) \rangle_{\text{pq}}. \quad (29)$$

Both $\rho(\theta)$ and $\langle \mathcal{O} \rangle_{\theta}$ are quantities calculable in the lattice simulation. The difficulty of the sign problem is now translated into the precise determination of the density of states; (21) implies that the phase quenched simulation at $\mu_q \neq 0$ with two degenerate flavours is identical to the simulation at finite isospin chemical potential $\mu_I (= \mu_q)$;

$$|\det F(\mu_q)|^2 = \det F(\mu_q) \det F(-\mu_q). \quad (30)$$

Then, the phase quenched expectation value goes through a qualitative change as μ_q increases; an exotic phase with pion condensation appears for $\mu_q > m_\pi/2$ [132]. For small μ_q , both lattice-QCD simulation [128] and an analysis in the χ PT [133, 134, 135] show that $\rho(\theta)$ behaves as Gaussian, while $\rho(\theta)$ becomes Lorentzian for $\mu_q > m_\pi/2$ in the χ PT. In the latter case, extremely precise determination of $\rho(\theta)$ and $\langle \mathcal{O} \rangle_\theta$ is crucially important. So far, the density of states method is applied for relatively small values of μ_q/T combined with the Taylor expansion of the fermion determinant [128, 136].

- *Complex Langevin method* — The sign problem arises from the importance sampling to deal with the multi-dimensional functional integral. Therefore, it may not appear in different quantization schemes other than the functional integral. The stochastic quantization [137, 138, 139, 140, 141] formulated in terms of the Langevin dynamics with a fictitious time is a promising candidate for such an alternative. If we consider a scalar field theory defined by an action $S[\phi]$, the Langevin equation reads

$$\frac{\partial \phi(x, s)}{\partial s} = -\frac{\delta S[\phi]}{\delta \phi(x, s)} + \eta(x, s), \quad (31)$$

where s is a fictitious time and η a Gaussian noise; $\langle \eta(x, s) \rangle = 0$ and $\langle \eta(x, s)\eta(x', s') \rangle = 2\delta(x - x')\delta(s - s')$. The expectation value is taken over the $\eta(x, s)$ distribution and the equilibrated value is obtained in the $s \rightarrow \infty$ limit. At finite μ_q the action and noise are complex. The complex Langevin dynamics can evade the sign problem and correctly describe the system at finite density for some simple models, while there are also cases where it may fall into a wrong answer [142, 143]. Whether this method is applicable to dense QCD or not is still an open question.

It would be an important milestone if the lattice-QCD simulation can show the existence/non-existence of the QCD critical point in μ_B - T plane. In [113, 144] the location of the Lee-Yang zero in the complex lattice-coupling ($\beta = 2N_c/g^2$) plane has been investigated using the multi-parameter reweighting for 2 + 1-flavour staggered fermions. If the thermal transition is of first order, the Lee-Yang zero nearest to the real axis in a finite lattice box is expected to approach to the real axis as the lattice volume increases, while there is no such tendency for the crossover transition. It was then concluded that the QCD critical point is located at $(\mu_B, T) = (\mu_E, T_E) = (360 \pm 40 \text{ MeV}, 162 \pm 2 \text{ MeV})$ for physical quark masses [144]. It has been argued, however, in [145] that the sign problem at finite baryon density can fool the Lee-Yang zero near the real axis. It is also suggested to study the behaviour of a set of Lee-Yang zeros in the complex β plane to make a firm conclusion.

If we *assume* that the convergence of the Taylor expansion in terms of μ_q/T is dictated by the singularity at the critical point, the radius of convergence is an indicator of the location of the critical point. In [116] it was reported that the coefficients up to sixth order yield $T_E/T_{pc} = 0.94 \pm 0.01$ and $\mu_E/T_{pc} = 1.8 \pm 0.1$ for 2-flavour staggered fermions with $m_\pi/m_\rho = 0.3$. In the same way, with 2 + 1-flavour staggered fermions, the radius of convergence is discussed in [146], though the results are not conclusive. The idea of the radius of convergence has been also tested in a chiral effective model coupled with the Polyakov loop, in which the exact location of the critical point and the higher-order coefficients are calculable in the mean-field approximation [147]. The result from the model test suggests that the relation between

the convergence radius of the expansion and the location of the critical point is not clear.

In [148] the canonical partition function is extracted using the density of states method with an assumption of the Gaussian distribution of the phase θ of the Dirac determinant. In this case the standard S-shape curve in the μ_B - n_B plane is a signature of the first-order transition. The location of the critical point is estimated to be $T_E/T_{pc} \approx 0.76$ and $\mu_E/T_{pc} \approx 7.5$ for 2-flavour staggered fermions with $m_\pi \simeq 770$ MeV. In [125] the canonical ensemble method is used to study the S-shape and it was found $T_E/T_{pc} = 0.94 \pm 0.03$ and $\mu_E/T_{pc} = 3.01 \pm 0.12$ for 3-flavour clover fermions with $m_\pi \simeq 700$ MeV.

As shown in figure 5 one may consider the critical surface $\mu_B = \mu_B(m_{ud}, m_s)$ and its behaviour near $\mu_B = 0$ to check whether the critical point is located in small μ_B region. In particular, on the $SU(3)_V$ symmetric line ($m_{ud} = m_s$), one can define the critical mass as a function of μ_q and make a Taylor expansion,

$$\frac{m_c(\mu_q)}{m_c(0)} = 1 + c_2 \left(\frac{\mu_q}{\pi T_{pc}} \right)^2 + c_4 \left(\frac{\mu_q}{\pi T_{pc}} \right)^4 + \dots \quad (32)$$

The sign of c_2 and c_4 determines whether the critical surface behaves like the standard scenario or the exotic scenario in figure 5. Simulations with 3-flavours of staggered fermions on a coarse lattice ($N_t = 4$) with the imaginary chemical potential method show $c_2 = -3.3(3)$ and $c_4 = -47(20)$ [149], which is consistent with the exotic scenario in figure 5. This does not, however, exclude a possibility that the critical point exists for large value of μ_q/T . Confirmation of this result with different fermion formulations with smaller lattice spacing is necessary to draw a firm conclusion [150].

In short summary, in any method, the validity of QCD simulations at finite baryon density is still limited in the region $\mu_q/T < 1$ at present because of the sign problem. Although some of the lattice-QCD simulations suggest the existence of the QCD critical point in μ_B - T plane, the results are to be taken with care if it is predicted at large μ_q/T .

5.2. Effective $U(1)_A$ symmetry restoration

For $N_f = 3$ the first-order transition at finite T is driven by the trilinear chiral condensates from the $U(1)_A$ -breaking KMT-type interaction with the strength c_0 as discussed in section 4.1. In the instanton calculation c_0 is proportional to the instanton density (18) which is screened by the medium at high T and μ_q as

$$n_{\text{inst}}(T, \mu_q) = \left(\frac{8\pi^2}{g^2} \right)^{2N_c} e^{-8\pi^2/g(\rho)^2} \rho^{-5} \exp \left[-\pi^2 \rho^2 T^2 \left(\frac{2N_c}{3} + \frac{N_f}{3} \right) - N_f \rho^2 \mu_q^2 \right], \quad (33)$$

in the one-loop calculation with the instanton size whose empirical value is $\rho \sim 0.3$ fm [151]. It is thus expected that the $U(1)_A$ -breaking interaction is exponentially suppressed as T and/or μ_q grow larger. If one performs the ρ -integration (which is not IR divergent thanks to the exponential suppression), the suppression factor would be T^{-14} or μ_q^{-14} for $N_c = N_f = 3$ by the dimensional reason. It is a non-trivial question whether the instanton-induced interaction drops by either exponential or power function [152]. The Columbia plot with an in-medium reduction of $U(1)_A$ breaking should have a smaller region for the first-order phase transition. This has been confirmed at $\mu_q = 0$ [153] in the Polyakov-loop extended chiral models such as the PNJL model [154, 155] and the PQM model [156]. Consequently the location of the QCD critical point at finite μ_q would be very sensitive to the strength c_0

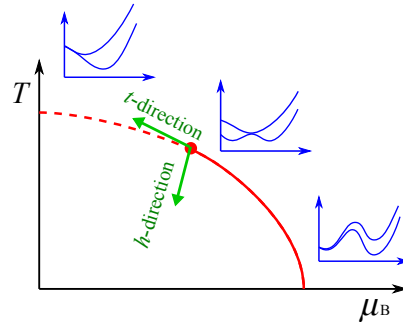


Figure 7. Schematic illustration of the potential shapes in the crossover, critical and first-order regions, respectively, from the left to the right. The t -direction at the critical point is tangential to the first-order phase boundary.

[153, 157, 158]. The negative coefficients c_2 and c_4 in (32) might be attributed to the effective $U(1)_A$ restoration at larger μ_q [159]; it has been found that the chiral model analysis with an exponential ansatz, $c_0 \propto e^{-N_f \rho^2 \mu_q^2}$, leads to a scenario similar to the right panel of figure 5.

5.3. QCD critical point search

In this subsection we summarize physical consequences of the critical point under the assumption that it exists in the QCD phase diagram.

Figure 7 is a schematic illustration of the shape of the effective potentials in the crossover and first-order transitions. If the critical point is approached along the first-order phase boundary, the associated potential shape looks like that of the second-order phase transition around a non-vanishing order parameter. The critical properties at the critical point can be mapped to the 3D Ising model with $Z(2)$ symmetry with the (reduced) temperature t and the external field h . On the μ_B - T plane in the QCD phase diagram the mapped t -direction is tangential to the first-order phase boundary because $Z(2)$ symmetry at the critical point is locally preserved along this direction. The determination of the h -direction, on the other hand, requires microscopic calculations.

In the vicinity of the critical point along the t -direction the correlation length ξ , the chiral condensate σ and the chiral susceptibility χ_σ have the following scaling;

$$\xi \sim t^{-\nu}, \quad \sigma = \langle \bar{\psi}\psi \rangle - \langle \bar{\psi}\psi \rangle_0 \sim t^\beta, \quad \chi_\sigma \sim t^{-\gamma}, \quad (34)$$

where $\nu \simeq 0.63$, $\beta \simeq 0.33$ and $\gamma \simeq 1.24$ are known critical exponents in the 3D Ising model. Because chiral symmetry is explicitly broken by $m_q \neq 0$, the chiral condensate at the critical point is non-vanishing and takes a finite $\langle \bar{\psi}\psi \rangle_0$. In the same way, along the h -direction, they scale as

$$\xi \sim h^{-\nu/\beta\delta}, \quad \sigma \sim h^{1/\delta}, \quad \chi_\sigma \sim h^{-1+1/\delta}, \quad (35)$$

where $\delta \simeq 4.8$. It is also possible to parametrize the singular part of the equation of state in a similar way as to the 3D Ising model [160].

The divergent correlation length ξ can be interpreted physically as the vanishing screening mass in the σ -meson channel, which may have significant consequences in the HIC experiments [49, 50]. However, one should keep in mind that the pole mass in the σ channel can never be massless since it is not directly related to ξ [161, 162].

In a finite-density medium there is a mixing between the chiral condensate and the baryon density. Therefore the divergence in the chiral susceptibility can be seen also in the baryon number susceptibility, leading to enhanced fluctuation in the baryon number $\langle(\delta N)^2\rangle$. It has been argued that the general moments (cumulants) become [163];

$$\langle(\delta N)^k\rangle_c \sim \xi^{k(5-\eta)/2-3}, \quad (36)$$

where $\langle\cdots\rangle_c$ represents the connected piece of the correlation function. Naturally the higher moments have stronger divergence in the vicinity of the critical point where $\xi \rightarrow \infty$. On the other hand, they require a large subtraction like $\langle(\delta N)^4\rangle - 3\langle(\delta N)^3\rangle$. It would be therefore more difficult to extract them accurately from HIC experiment data.

Here we emphasize that the soft mode responsible for the critical property at the critical point is the density fluctuation rather than the chiral fluctuation. To see this point it is useful to consider the following Ginzburg-Landau expansion [164, 165];

$$F[\sigma, \rho] = -\frac{\omega^2}{\Gamma}\sigma^2 - \frac{i\omega}{\lambda\mathbf{q}^2}\rho^2 + V[\sigma, \rho] \quad (37)$$

$$V[\sigma, \rho] = a\sigma^2 + b\sigma^4 + c\sigma^6 - h\sigma + \gamma\sigma^2\rho + \frac{1}{2}\rho^2 - j\rho. \quad (38)$$

Here ρ represents one of conserved charge densities such as the baryon density n_B with an appropriate normalization. The equilibrium values of σ and ρ are fixed by $\partial V/\partial\sigma = 0$ and $\partial V/\partial\rho = 0$. The dynamics is solved by the kinetic equations of motion $\partial F/\partial\sigma = 0$ and $\partial F/\partial\rho = 0$, which leads to the eigen-frequencies [165],

$$\chi_\sigma^{-1} = \frac{\omega_\sigma^2}{\Gamma} = \chi_h^{-1} + 4\gamma^2\sigma^2, \quad \chi_\rho^{-1} = \frac{i\omega_\rho}{\lambda\mathbf{q}^2} = \frac{\chi_h^{-1}}{\chi_h^{-1} + 4\gamma^2\sigma^2}, \quad (39)$$

where ω_σ and ω_ρ are eigen-frequencies which are identified as the chiral and density modes, respectively. The notation χ_h represents the chiral susceptibility without the density mixing taken into account, which diverges at the critical point. It is apparent from the above expressions that the soft mode at the QCD critical point is the density fluctuation and the σ mode is a decoupled fast mode. This also explains in a natural way why only the screening mass of the σ meson becomes vanishing at the critical point, while the pole mass never does as mentioned above [162].

5.4. First-order phase transition at high baryon density

We now turn to the chiral phase transition at low temperature and high baryon density where lattice simulations are not reachable yet. In this region, only qualitative analyses based on various chiral effective theories are available at present. Many of these models predict a first-order transition in cold and dense matter; we are going to extract some common feature in these models based on a quasi-particle picture at $\mu_q \neq 0$.

Let us introduce a vacuum pressure $P_{\text{vac}}[M_q]$, which embodies the dynamical chiral symmetry breaking, as a function of M_q (constituent quark mass) as

$$P_{\text{vac}}[M_q] = -a(M_0^2 - M_q^2)^2, \quad (40)$$

with a positive curvature parameter a . The maximum of $P_{\text{vac}}[M_q]$ is realized when $M_q = \pm M_0 \neq 0$. (If the current quark mass m_q is non-zero, a linear term in M_q , which favours $M_q > 0$ at the maximum of $P_{\text{vac}}[M_q]$, should be present.) At zero temperature, as long as μ_q is smaller than M_q , nothing happens and the vacuum

remains empty, while n_B starts arising for $\mu_q > M_q$. The pressure from finite μ_q is expressed as

$$P_\mu[M_q] = \int_0^{\mu_q} d\mu'_q n_q(\mu'_q) = \frac{\nu}{6\pi^2} \int_0^{\mu_q} d\mu'_q (\mu_q'^2 - M_q^2)^{3/2} \theta(\mu_q'^2 - M_q^2), \quad (41)$$

where $n_q(\mu_q)$ represents the fermion density in the quasi-particle approximation and $\nu = (\text{spin}) \times (\text{colour}) \times (\text{flavour})$ is the fermion degeneracy. Because more particles can reside in the Fermi sphere for smaller mass, $P_\mu[M_q]$ naturally has a maximum at $M_q = 0$ and goes to zero at $M_q = \mu_q$.

Here $P_{\text{vac}}[M_q]$ and $P_\mu[M_q]$ have a peak at $M_q = M_0$ and $M_q = 0$, respectively. Assuming that the total pressure is simply $P[M_q] = P_{\text{vac}}[M_q] + P_\mu[M_q]$, we can see that the existence of two separate peaks in $P[M_q]$ requires [166],

$$a < \frac{\nu}{16\pi^2} \frac{\mu_q^2}{M_0^2} \lesssim \frac{\nu}{16\pi^2} \simeq 0.076, \quad (42)$$

for 2-flavour case with $\nu = 12$. At the first-order critical point the peak at $M_q = 0$ is just as high as the second peak at $M_q \simeq M_0$, which determines the critical chemical potential,

$$a \simeq \frac{\nu}{24\pi^2} \frac{\mu_c^4}{M_0^4}. \quad (43)$$

Once a satisfies (42), the chiral phase transition with increasing μ_q at $T = 0$ should be of first order at $\mu_q \simeq \mu_c$.

The actual value of a is model-dependent: In the NJL model with two flavours and in the linear- σ model, a is estimated respectively as

$$a = \begin{cases} \frac{1}{2M_0^2} \left(\frac{\nu\Lambda^2}{8\pi^2} - \frac{1}{4G_S} \right) = 0.067 & \text{(NJL model)} \\ \frac{M_\sigma^2 f_\pi^2}{8M_0^4} = 0.02 \sim 0.05 & \text{(linear-}\sigma \text{ model)} \end{cases}, \quad (44)$$

where we used the standard NJL parameters; $\Lambda = 631$ MeV, $G_S \Lambda^2 = 2.19$, and the resultant $M_0 = 336.2$ MeV [10]. The uncertainty in the linear- σ model comes from the choice of the σ meson mass. Then, in both cases, the estimated a satisfies the inequality (42) implying the first-order phase transition. The critical chemical potential deduced from (43) is, in the NJL model case, given by $\mu_c = 1.07M_0 \simeq 360$ MeV which is consistent with that obtained numerically in the NJL model.

Let us now argue that the first-order transition obtained as above is rather sensitive to the choice of the model Lagrangian. Indeed, it has been known that the repulsive contribution to the pressure of the form $+G_V n_q^2$ induced by a quark interaction of density-density type can totally wash out the first-order transition [167, 168, 169, 170, 171, 166]. For example, in the NJL model with the density-density interaction, the condition (42) is changed to

$$a < \frac{\nu}{16\pi^2} \left(1 - \frac{2\nu G_V \mu_q^2}{3\pi^2} \right), \quad (45)$$

which implies that the first-order phase transition does not arise for $G_V > 0.25G_S$ [169, 170, 166].

6. Formation of the diquark condensate

Finding a ground state of quark matter at $T \approx 0$ with extremely large value of μ_q is an interesting theoretical challenge. (We use μ_q instead of μ_B throughout this section, for our central interest is the quark degrees of freedom). Let us consider the Cooper's stability-test in quark matter [60, 61]. In the perturbative regime of QCD the one-gluon exchange potential is proportional to a product of the quark $SU(N_c)$ charges;

$$(t^a)_{\alpha\beta}(t^a)_{\alpha'\beta'} = -\frac{N_c + 1}{4N_c}(\delta_{\alpha\beta}\delta_{\alpha'\beta'} - \delta_{\alpha\beta'}\delta_{\alpha'\beta}) + \frac{N_c - 1}{4N_c}(\delta_{\alpha\beta}\delta_{\alpha'\beta'} + \delta_{\alpha\beta'}\delta_{\alpha'\beta}). \quad (46)$$

The first term in the right-hand side of (46) with negative sign is anti-symmetric under the exchange of colour indices; $\alpha \leftrightarrow \alpha'$ or $\beta \leftrightarrow \beta'$, so that a quark pair in the colour anti-triplet channel has attraction. The second term in the right-hand side of (46) with positive sign is symmetric under the same exchange of colour indices, so that a quark pair in the colour sextet channel has repulsion. Fermi system with two particles attracting each other on a sharp Fermi sphere has an instability towards the formation of Cooper pairs. Therefore, normal quark matter inevitably becomes colour-superconducting (CSC) phase with diquark condensate at asymptotic high density and at sufficiently low temperature [60, 61, 172, 173, 174].

Since quarks carry not only spin but also colour and flavour, various pairing patterns are possible. Hereafter we use the following notation; the colour indices α, β, γ run from 1 to 3 meaning r (red), g (green) and b (blue) in order, and in the same way the flavour indices i, j, k run from 1 to 3 meaning u (up), d (down) and s (strange) in order. We will focus our attention to quark matter below the charm threshold, i.e. $\mu_q < m_{\text{charm}}$, so that we do not take into account heavy flavours (c, b and t).

Spin-zero condensate: The quark pairing with zero total spin is characterized by the following order parameter with 3×3 matrix structure [88];

$$(d^\dagger)_{\alpha i} \sim \epsilon_{\alpha\beta\gamma} \epsilon_{ijk} \langle \psi_{\beta j}^\dagger C \gamma^5 \psi_{\gamma k} \rangle. \quad (47)$$

The quark pair in this case is in the colour anti-symmetric (anti-triplet), flavour anti-symmetric (anti-triplet) and spin anti-symmetric channel to satisfy the Fermi statistics. The charge conjugation matrix $C = i\gamma^2\gamma^0$ together with γ^5 makes the above condensate a Lorentz scalar. (The effect of instantons and also quark masses favours the scalar condensate instead of the pseudo-scalar condensate.) If the masses of u, d and s quarks are all degenerate, there is an exact flavour $SU_V(3)$ symmetry. Then, one can always diagonalize the order parameter by the bi-unitary rotation in colour and flavour space to obtain $(d)_{i\alpha} = \delta_{i\alpha}\Delta_i$. We will adopt this as an ansatz even when u, d and s quarks are not degenerate, which is in practise a good approximation [175, 176].

Let us introduce a notation $\Delta_{ds} = \Delta_1, \Delta_{su} = \Delta_2, \Delta_{ud} = \Delta_3$ to indicate which quarks are involved in the Cooper pairing. If all the gaps are non-vanishing ($\Delta_{ud} \neq 0, \Delta_{ds} \neq 0$ and $\Delta_{su} \neq 0$), such a state is called the colour-flavour locked (CFL) phase [88] because the colour and flavour degrees of freedom are entangled with each other. For $\Delta_{ds} = 0$ with other components non-vanishing, it is called the uSC phase since both Δ_{ud} and Δ_{su} contain the u quark. The dSC and sSC phases are defined in the same way [177, 176, 178]. If only Δ_{ud} is non-vanishing, it is called the 2SC (two-flavour superconducting) phase. In case that we refer to similar phases with other flavour

Pairing	CFL	uSC	dSC	sSC	2SC	2SCds	2SCsu	NQM
Δ_{ud}	○	○	○	×	○	×	×	×
Δ_{ds}	○	×	○	○	×	○	×	×
Δ_{su}	○	○	×	○	×	×	○	×

Table 3. Classification of the colour-superconducting phases.

combination, we write the 2SCds, 2SCsu or 2SCud(=2SC) phase [175, 179]. When all the pairing gaps are absent, the system is in the state of normal quark matter (NQM). We summarize these abbreviations in table 3.

Let us now consider the symmetry breaking patterns ($\mathcal{G} \rightarrow \mathcal{H}$) in the CFL and 2SC phases. * In the CFL phase for massless 3-flavours, one finds the following pattern [88, 15],

$$\mathcal{G} = \text{SU}(3)_C \times \underbrace{\text{SU}(3)_L \times \text{SU}(3)_R}_{\supset \text{U}(1)_{\text{em}}} \times \text{U}(1)_B \times \text{Z}(6)_A, \quad (48)$$

$$\mathcal{H} = \underbrace{\text{SU}(3)_{C+L+R}}_{\supset \text{U}(1)_{\text{em}+C}} \times \text{Z}(2)_V. \quad (49)$$

Here the baryon number symmetry is broken to leave its discrete subgroup $\text{Z}(2)_V$ which corresponds to a reflection $\psi \rightarrow -\psi$. Also, (global) colour symmetry and chiral symmetry are broken simultaneously to leave their diagonal subgroup $\text{SU}(3)_{C+L+R}$ intact. Note that the electromagnetic symmetry $\text{U}(1)_{\text{em}}$ associated with the electric charge $Q = \text{diag}(2/3, -1/3, -1/3)$ happens to be a subgroup of the vector symmetry $\text{SU}(3)_{L+R}$. In the CFL phase $\text{U}(1)_{\text{em}}$ survives as a *modified* symmetry, $\text{U}(1)_{\text{em}+C}$, which contains simultaneous electromagnetic and colour rotation. As a result, seven gluons and one gluon-photon mixture acquire finite Meissner mass by the Anderson-Higgs mechanism, while the other photon-gluon mixture remains massless.

The 2SC phase is quite different from the CFL phase in the sense that only u and d quarks participate in the pairing with a chiral flavour-singlet combination. The symmetry breaking pattern in this case for massless 2-flavours with infinitely heavy strange quarks reads [15],

$$\mathcal{G} = \text{SU}(3)_C \times \underbrace{\text{SU}(2)_L \times \text{SU}(2)_R}_{\supset \text{U}(1)_{\text{em}}} \times \text{U}(1)_B \times \text{Z}(4)_A, \quad (50)$$

$$\mathcal{H} = \text{SU}(2)_C \times \underbrace{\text{SU}(2)_L \times \text{SU}(2)_R}_{\supset \text{U}(1)_{\text{em}+C}} \times \text{U}(1)_{C+B}. \quad (51)$$

Note that chiral symmetry remains intact while colour symmetry is broken, so that five gluons (4th to 8th) receive finite Meissner mass. In the 2SC phase, the baryon-number symmetry $\text{U}(1)_B$ survives as a *modified* symmetry, $\text{U}(1)_{C+B}$, which contains simultaneous electromagnetic and 8-th colour rotation. The global electromagnetism which is originally a combination of the baryon number symmetry and the isospin symmetry, survives also as a *modified* symmetry, $\text{U}(1)_{\text{em}+C}$. Therefore, the 2SC phase is neither a superfluid nor an electromagnetic superconductor. The modified symmetries discussed above remain unbroken in the uSC and dSC phases as well.

* Similar comment on the quotient groups (\mathcal{G}' and \mathcal{H}') as given to (9) and (10) is applied here.

The CFL phase is reminiscent of what is called the B phase of superfluid ${}^3\text{He}$ in which fermionic ${}^3\text{He}$ atoms have a spin-triplet ($S = 1$) and p -wave ($L = 1$) pairing. The B phase is a state in which the orbital angular momentum \mathbf{L} and the spin \mathbf{S} are locked so that the symmetry breaking pattern is $\text{SO}(3)_S \times \text{SO}(3)_L \times \text{U}(1)_\phi \rightarrow \text{SO}(3)_{S+L}$, where $\text{U}(1)_\phi$ is a symmetry corresponding to $\text{U}(1)_B$ in quark matter.

Spin-one condensate: There is also a possibility of flavour symmetric Cooper pairs such as the pairing within the same flavour [172]. In this case s -wave Cooper pair must be spin triplet ($J = L + S = 0 + 1 = 1$) to satisfy the Fermi statistics.

Various forms of the spin-one CSC states have been studied so far [179, 180, 181, 182]. Since the Cooper pair is triplet in both colour and spin, the order parameter becomes a complex 3×3 matrix, which is similar to the situation in the CFL phase where the Cooper pair is triplet in both colour and flavour. The explicit form would be

$$(\tilde{d}^\dagger)_{\alpha i} \sim \epsilon_{\alpha\beta\gamma} \langle \psi_\beta^\dagger C \gamma^i \psi_\gamma \rangle, \quad (52)$$

where i refers to not the flavour but the Lorentz index. The colour-spin locked (CSL) ansatz, $(\tilde{d})_{i\alpha} \propto \delta_{i\alpha}$, leads to a symmetry breaking pattern which is similar to the CFL phase in CSC and to the B phase in superfluid ${}^3\text{He}$;

$$\text{SU}(3)_C \times \text{SU}(2)_J \times \text{U}(1)_{\text{em}} \rightarrow \text{SU}(2)_{C+J}. \quad (53)$$

On the other hand, if we take an ansatz, $(\tilde{d})_{\alpha i} \propto \delta_{\alpha 3}(\delta_{i1} + i\delta_{i2})$, we have a symmetry breaking pattern,

$$\text{SU}(3)_C \times \text{SU}(2)_J \times \text{U}(1)_{\text{em}} \rightarrow \text{SU}(2)_C \times \text{U}_{J+\text{em}} \times \text{U}(1)_{\text{em}+C}, \quad (54)$$

which is analogous to the A phase of superfluid ${}^3\text{He}$ in which the symmetry breaking pattern is; $\text{SO}(3)_S \times \text{SO}(3)_L \times \text{U}(1)_\phi \rightarrow \text{U}(1)_{S_z} \times \text{U}(1)_{L_z+\phi}$. Other pairing patterns such as the polar phase, the planar phase and so on have been also investigated [182].

Weak-coupling results: In the asymptotically high-density region, the running coupling constant of the strong interaction becomes small enough to justify the weak-coupling calculations, so that the diquark condensate as well as the gap energy of quarks can be estimated from the first-principle QCD calculation. The driving force of the diquark condensate is the interaction between quarks due to gluon exchange. The chromoelectric part of the interaction in high-density quark matter is screened by the Debye mass $m_D = \sqrt{N_f/(2\pi^2)} g \mu_q$, while the chromomagnetic part of the interaction is screened only dynamically by Landau damping [183]. Therefore, instead of having the standard BCS form, $\Delta \sim \mu_q \exp(-\text{const.}/g^2)$, the gap energy at the Fermi surface is parametrically enhanced due to large forward scattering between quarks [183, 184, 185, 186, 180];

$$\Delta_F = 512\pi^4 \left(\frac{2}{N_f} \right)^{5/2} e^{-(\pi^2+4)/8} (\lambda_1^{a_1} \lambda_2^{a_2})^{-1/2} g^{-5} \mu_q \exp\left(-\frac{3\pi^2}{\sqrt{2}g} \right), \quad (55)$$

where $\lambda_1 = a_1 = 1$ and $\lambda_2 = a_2 = 0$ for the 2SC phase, while $\lambda_1 = 4$ and $\lambda_2 = 1$ with $a_1 = 1/3$ and $a_2 = 2/3$ in the CFL phase. In the exponent of (55), unusual dependence on the coupling g^{-1} instead of the standard dependence g^{-2} enhances the gap substantially in the weak coupling regime both for 2SC and CFL phases. We see that $\Delta^{2\text{SC}}$ in the 2SC phase is greater than that in the CFL phase as $\Delta^{2\text{SC}} = 2^{1/3} \Delta^{\text{CFL}}$, which holds not only in the weak-coupling QCD calculation but also in effective model

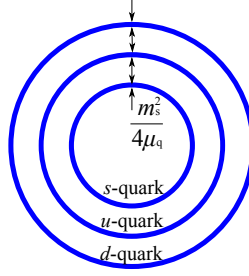


Figure 8. Fermi surface mismatch in unpaired normal quark matter.

calculations. Similarly to the BCS theory, the gap energy at zero temperature and the critical temperature are related to each other in the mean-field approximation [180],

$$T_c = (\lambda_1^{a_1} \lambda_2^{a_2})^{1/2} \frac{e^\gamma}{\pi} \Delta_F. \quad (56)$$

Note that the factor $(\lambda_1^{a_1} \lambda_2^{a_2})$ in the right-hand side is cancelled by the same factor in (55), so that $\Delta^{2\text{SC}} > \Delta^{\text{CFL}}$ does not necessary imply $T_c^{2\text{SC}} > T_c^{\text{CFL}}$.

6.1. Neutrality in electric and colour charges

For the bulk system to be stable, the total electric and colour charges must be zero due to the Gauss law [187, 188, 189]. In some effective models which do not have gauge fields as explicit degrees of freedom, the charge neutrality must be imposed by electric and colour chemical potentials, $\mu_{\alpha i} = \mu_q + \mu_Q(Q)_{ii} + \mu_3(T_3)_{\alpha\alpha} + \mu_8(\frac{2}{\sqrt{3}}T_8)_{\alpha\alpha}$. Their explicit forms read

$$\begin{aligned} \mu_{ru} &= \mu_q - \frac{2}{3}\mu_e + \frac{1}{2}\mu_3 + \frac{1}{3}\mu_8, & \mu_{gd} &= \mu_q + \frac{1}{3}\mu_e - \frac{1}{2}\mu_3 + \frac{1}{3}\mu_8, \\ \mu_{bs} &= \mu_q + \frac{1}{3}\mu_e - \frac{2}{3}\mu_8, & \mu_{rd} &= \mu_q + \frac{1}{3}\mu_e + \frac{1}{2}\mu_3 + \frac{1}{3}\mu_8, \\ \mu_{gu} &= \mu_q - \frac{2}{3}\mu_e - \frac{1}{2}\mu_3 + \frac{1}{3}\mu_8, & \mu_{rs} &= \mu_q + \frac{1}{3}\mu_e + \frac{1}{2}\mu_3 + \frac{1}{3}\mu_8, \\ \mu_{bu} &= \mu_q - \frac{2}{3}\mu_e - \frac{2}{3}\mu_8, & \mu_{gs} &= \mu_q + \frac{1}{3}\mu_e - \frac{1}{2}\mu_3 + \frac{1}{3}\mu_8, \\ \mu_{bd} &= \mu_q + \frac{1}{3}\mu_e - \frac{2}{3}\mu_8, \end{aligned} \quad (57)$$

where the electron chemical potential μ_e satisfies $\mu_e = -\mu_Q$ due to β -equilibrium. These constraints add some varieties in the physics of CSC because one needs to consider the Cooper pairing between quarks with mismatched Fermi surfaces.

For unpaired quark matter with $m_{ud} = 0$ and $m_s \neq 0$, the number of strange quarks is less than that of other quarks. There arise electrons in the system to maintain charge neutrality accordingly. The neutrality conditions obtained by the variation of the free energy, $\partial\Omega_{\text{unpaired}}/\partial\mu_e = \partial\Omega_{\text{unpaired}}/\partial\mu_3 = \partial\Omega_{\text{unpaired}}/\partial\mu_8 = 0$, lead to $\mu_3 = \mu_8 = 0$ and $\mu_e = m_s^2/(4\mu_q)$. With the free dispersion relation at large chemical potential, $\epsilon_{ud}(p) = |\mathbf{p}|$ and $\epsilon_s(p) = \sqrt{|\mathbf{p}|^2 + m_s^2} \simeq |\mathbf{p}| + m_s^2/(2\mu_q)$, the Fermi momenta have mismatches as

$$p_F^u = \mu_q - \frac{m_s^2}{6\mu_q}, \quad p_F^d = \mu_q + \frac{m_s^2}{12\mu_q}, \quad p_F^s = \mu_q - \frac{5m_s^2}{12\mu_q}. \quad (58)$$

This is illustrated in figure 8.

At high density where the expansions in terms of m_s/μ_q and Δ/μ_q are valid, model-independent conclusions can be drawn for the CSC quark matter at $T = 0$

[187, 188]. In the CFL phase the modified electric charge \tilde{Q} associated with the symmetry $U(1)_{\text{em}+C}$ is conserved. Also, all the Cooper pairs have $\tilde{Q} = 0$, so that the CFL quark matter at $T = 0$ is a \tilde{Q} -insulator [190]. Thus, the CFL free energy Ω_{CFL} is independent of the corresponding chemical potential except for a small contribution proportional to μ_e^4 from \tilde{Q} -violating electrons. Under the neutrality conditions, $\partial\Omega_{\text{CFL}}/\partial\mu_e = \partial\Omega_{\text{CFL}}/\partial\mu_3 = \partial\Omega_{\text{CFL}}/\partial\mu_8 = 0$, we obtain

$$\mu_3 = \mu_e, \quad \mu_8 = \frac{1}{2}\mu_e - \frac{m_s^2}{2\mu_q}, \quad \mu_e = 0. \quad (59)$$

It is an important property that the CFL phase ($\Delta_{ud} \simeq \Delta_{ds} \simeq \Delta_{su}$ with $\mu_e = 0$) is rigid against the Fermi surface mismatch [190] as long as the CFL phase is in the stable region; $\Delta > m_s^2/(2\mu_q)$. We will discuss later what happens once this stability condition is violated in section 7.2.

In the 2SC phase the colour and charge neutralities lead to

$$\mu_3 = \mu_8 = 0, \quad \mu_e = \frac{m_s^2}{2\mu_q}, \quad (60)$$

so that electrons are required to be present with even larger chemical potential than the normal quark matter. Also, the 2SC phase contains ungapped \tilde{Q} -carrying modes, and is therefore a \tilde{Q} -conductor.

6.2. Ginzburg-Landau approach

To identify the phase structure of CSC near second-order or weak first-order transitions at finite T , the Ginzburg-Landau approach is quite useful [61, 191]. If we assume that the gap energy is small compared to the critical temperature, the Ginzburg-Landau free energy with a power series expansion in terms of $(d)_{i\alpha}$ up to the quartic order reads [177],

$$\begin{aligned} \Omega = & \alpha \text{tr} dd^\dagger + \beta_1 (\text{tr} dd^\dagger)^2 + \beta_2 \text{tr}(dd^\dagger)^2 \\ & + \epsilon \sum_\alpha (|d_{\alpha u}|^2 + |d_{\alpha d}|^2) + \frac{\eta}{3} \sum_\alpha (|d_{\alpha d}|^2 + |d_{\alpha s}|^2 - 2|d_{\alpha u}|^2), \end{aligned} \quad (61)$$

where tr is taken in flavour space. For $m_s = \mu_e = 0$ the transition from the CFL phase to normal quark matter is driven by the parameter α changing the sign from negative to positive. The fourth term with ϵ takes care of the asymmetry between (u, d) and s introduced by $m_s \neq 0$, while the fifth term with η represents the asymmetry between u and (d, s) from the charge neutrality effect by $\mu_e \neq 0$. The effect of colour neutrality is negligible near T_c . Under the diagonal ansatz on the gap matrix, the free energy simplifies into

$$\begin{aligned} \Omega = & \alpha' (\Delta_{ud}^2 + \Delta_{ds}^2 + \Delta_{su}^2) - \epsilon \Delta_{ud}^2 - \eta \Delta_{ds}^2 \\ & + \beta_1 (\Delta_{ud}^2 + \Delta_{ds}^2 + \Delta_{su}^2)^2 + \beta_2 (\Delta_{ud}^4 + \Delta_{ds}^4 + \Delta_{su}^4) \end{aligned} \quad (62)$$

with $\alpha' = \alpha + \epsilon + \eta/3$. In the weak-coupling analysis one can show that $\beta_1 = \beta_2 = \beta$ and $\alpha = \alpha_0(T - T_c)/T_c$, where $\alpha_0 = 2\mu_q^2/\pi^2$ and T_c is the critical temperature defined for $\epsilon = \eta = 0$. In the weak-coupling limit of QCD with $m_s \ll \mu_q$, it is shown that $\epsilon \simeq 2\eta \simeq 2\alpha_0\delta$ with a parameter $\delta \simeq (m_s^2/8\mu_q^2) \ln(\mu_q/T_c)$. Then the gap energies near T_c behave as

$$\Delta_{ud}^2(T) = \frac{\alpha_0}{8\beta} \left(\frac{T_c - T}{T_c} + \frac{8}{3}\delta \right), \quad \Delta_{ds}^2(T) = \Delta_{ud}^2 - \frac{\alpha_0\delta}{2\beta}, \quad \Delta_{su}^2(T) = \Delta_{ud}^2 - \frac{\alpha_0\delta}{\beta}. \quad (63)$$

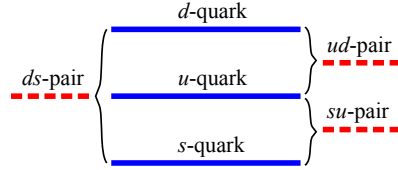


Figure 9. Ordering of the averaged Fermi surfaces for respective Cooper pairs.

The inequalities, $\Delta_{ud}(T) > \Delta_{ds}(T) > \Delta_{su}(T)$, imply sequential melting of CSC as T increases at high baryon density, i.e. CFL \rightarrow dSC \rightarrow 2SC \rightarrow NQM. This scenario of melting pattern has been confirmed by explicit calculations in the NJL model [178].

The ordering $\Delta_{ud} > \Delta_{ds} > \Delta_{su}$ in (63) can be understood in an intuitive manner. Because T is close to T_c , the Fermi surface is blurred and the mismatch of the Fermi momentum no longer imposes a pressure to take the pairing apart. The magnitude of the gap energy is then determined by the density of states. For example, the magnitude of the density of states for the pairing Δ_{ud} is related to the size of the “averaged” Fermi surface over u and d quarks. The Fermi surface ordering as shown in figure 8 gives rise to the ordering of the averaged Fermi surfaces as shown in figure 9, which explains the ordering $\Delta_{ud} > \Delta_{ds} > \Delta_{su}$ near T_c .

In some model calculations in the literature, uSC instead of dSC appears even for extremely large μ_q . This is caused by an artifact of the UV cutoff Λ in the model: If Λ is not chosen to be sufficiently large, ϵ and η suffer from significant cutoff-artifact, so that η may even have an opposite sign from the QCD prediction [178]. On the other hand, as μ_q becomes small and approaches to m_s , the expansion in terms of m_s/μ_q adopted for the computation of ϵ and η in (61) is no longer valid, and the other melting pattern, CFL \rightarrow uSC \rightarrow 2SC \rightarrow NQM, indeed becomes possible [178].

6.3. Quark-hadron continuity and $U(1)_A$ anomaly

The Ginzburg-Landau approach can be extended to incorporate the competition between the diquark condensate and the chiral condensate [192]. In this case it is necessary to distinguish the right-handed and left-handed diquark condensates d_L and d_R as given in (13) to construct properly the Ginzburg-Landau free energy with the symmetry \mathcal{G} in (48). The basic transformation properties of the fields Φ , d_L and d_R are

$$\Phi \rightarrow V_L \Phi V_R^\dagger, \quad d_L \rightarrow V_L d_L V_C^t, \quad d_R \rightarrow V_R d_R V_C^t, \quad (64)$$

where V_L , V_R and V_C correspond to $U(3)_L$, $U(3)_R$ and $SU(3)_C$ rotations, respectively.

In a simple case where all u , d and s quarks are massless, the chiral part has a standard expansion in the same form as (16);

$$\Omega_\Phi = \frac{a_0}{2} \text{tr} \Phi^\dagger \Phi + \frac{b_1}{4!} (\text{tr} \Phi^\dagger \Phi)^2 + \frac{b_2}{4!} \text{tr} (\Phi^\dagger \Phi)^2 - \frac{c_0}{2} (\det \Phi + \det \Phi^\dagger). \quad (65)$$

The term with the coefficient c_0 originates from the axial anomaly.

The diquark free energy up to the quartic order reads

$$\begin{aligned} \Omega_d = & \alpha \text{tr} (d_L d_L^\dagger + d_R d_R^\dagger) + \beta_1 \left[(\text{tr} d_L d_L^\dagger)^2 + (\text{tr} d_R d_R^\dagger)^2 \right] \\ & + \beta_2 \left[\text{tr} (d_L d_L^\dagger)^2 + \text{tr} (d_R d_R^\dagger)^2 \right] \end{aligned}$$

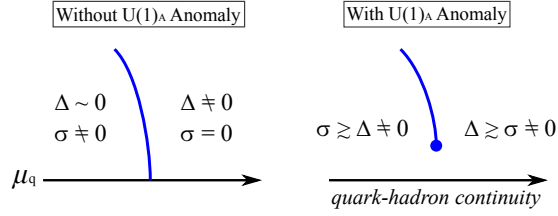


Figure 10. Schematic figure on the realization of the quark-hadron continuity induced by the $U(1)_A$ anomaly. (Left) First-order phase boundary near $T = 0$ without the anomaly-induced $\sigma\Delta^2$ term. (Right) Smooth crossover and the appearance of a critical point due to a large $\sigma\Delta^2$ term with $\gamma > 0$ in (68).

$$+ \beta_3 \text{tr}(d_R d_L^\dagger d_L d_R^\dagger) + \beta_4 \text{tr} d_L d_L^\dagger \text{tr} d_R d_R^\dagger. \quad (66)$$

The transition from the CFL phase to normal quark matter is driven by the parameter α changing the sign from negative to positive. Unlike $\det \Phi$ in (65), terms such as $\det d_L$ and $\det d_R$ are not allowed in (66) since they break $U(1)_B$.

The coupling between the diquark and the chiral condensates has the following general form up to the quartic order;

$$\begin{aligned} \Omega_{\Phi d} = & \gamma_1 \text{tr}(d_R d_L^\dagger \Phi + d_L d_R^\dagger \Phi^\dagger) \\ & + \lambda_1 \text{tr}(d_L d_L^\dagger \Phi \Phi^\dagger + d_R d_R^\dagger \Phi^\dagger \Phi) + \lambda_2 \text{tr}(d_L d_L^\dagger + d_R d_R^\dagger) \text{tr} \Phi^\dagger \Phi \\ & + \lambda_3 (\det \Phi \text{tr} d_L d_R^\dagger \Phi^{-1} + \det \Phi^\dagger \text{tr} d_R d_L^\dagger \Phi^t). \end{aligned} \quad (67)$$

The term with the coefficient γ_1 originates from the axial anomaly.

In the massless 3-flavour limit, one may assume $\Phi = \text{diag}(\sigma, \sigma, \sigma)$ and $d_L = -d_R = \text{diag}(\Delta, \Delta, \Delta)$ and then the sum of above three pieces amounts to

$$\Omega_{3F} = \left(\frac{a}{2} \sigma^2 - \frac{c}{3} \sigma^3 + \frac{b}{4} \sigma^4 \right) + \left(\frac{\alpha}{2} \Delta^2 + \frac{\beta}{4} \Delta^4 \right) - \gamma \Delta^2 \sigma + \lambda \Delta^2 \sigma^2. \quad (68)$$

Here the σ^3 and the $\Delta^2 \sigma$ terms originate from the axial anomaly. From the Fierz transform of the anomaly-induced KMT interaction in the quark level, the coefficients c and γ turn out to have the same sign [192]. Furthermore, the sign of c and γ can be taken to be positive without loss of generality because of the relation, $\Omega_{3F}(\sigma, \Delta; c, \gamma) = \Omega_{3F}(-\sigma, \Delta; -c, -\gamma)$, which is a situation analogous to the quark mass term.

It should be noted that the $\Delta^2 \sigma$ term with positive coefficient γ favours the coexistence of the chiral and diquark condensates. Also, this term is linear in σ and behaves as if it is an explicit chiral symmetry breaking term. In contrast, $\Delta^2 \sigma^2$ term with positive coefficient λ (the positive sign is supported by the weak-coupling calculation and in the NJL model) disfavours the coexistence. Therefore, if the effect of γ is sufficiently strong and Δ is sufficiently large, the first-order phase boundary, which normally separates the chiral symmetry breaking phase ($\sigma \neq 0$) and the CFL phase ($\sigma = 0$ and $\Delta \neq 0$), can be smeared out. In such a case the two phases are connected smoothly to each other and a critical point associated with this crossover appears as shown in figure 10.

The smooth crossover of the CFL phase and the Nambu-Goldstone (hadronic) phase may have a close connection to the idea of *quark-hadron continuity* [175, 193]. Since the axial anomaly tends to enhance (reduce) the first-order transition through

the term proportional to c (γ) in (68), it is a dynamical issue whether the phase diagram as sketched in figure 10 is realized or not in the real world [194, 195, 196].

6.4. Collective excitations

An interesting and related question associated with the $U(1)_A$ anomaly is the fate of collective excitations. Using the chiral effective Lagrangian approach [197], one finds the dispersion relations for the pions and kaons in the CFL phase with $m_s \neq 0$ and $\mu_e \neq 0$ [198, 199],

$$\begin{aligned}\epsilon_{\pi^\pm}(p) &= \pm\mu_e + \sqrt{v^2 p^2 + M_{\pi^\pm}^2}, \\ \epsilon_{K^\pm}(p) &= \pm\mu_e \mp \frac{m_s^2}{2\mu_q} + \sqrt{v^2 p^2 + M_{K^\pm}^2}, \\ \epsilon_{K^0}(p) &= -\frac{m_s^2}{2\mu_q} + \sqrt{v^2 p^2 + M_{K^0}^2},\end{aligned}\tag{69}$$

where $v^2 = 1/3$ at high density. The CFL-meson masses are given by

$$\begin{aligned}M_{\pi^\pm}^2 &= a(m_u + m_d)m_s + \chi(m_u + m_d), \\ M_{K^\pm}^2 &= a(m_u + m_s)m_d + \chi(m_u + m_s), \\ M_{K^0}^2 &= a(m_d + m_s)m_u + \chi(m_d + m_s).\end{aligned}\tag{70}$$

Here $a = 3\Delta^2/(\pi^2 f_\pi^2)$ with $f_\pi^2 = (21 - 8 \ln 2)\mu_q^2/(36\pi^2)$ at high density and χ parametrizes the contribution of the $U(1)_A$ anomaly which generates $\langle \bar{\psi}\psi \rangle$ and therefore contributes to the CFL-meson masses.

In the absence of the $U(1)_A$ -breaking term ($\chi = 0$), the energies for K^+ and K^0 become negative and kaon condensation occurs for $m_s \gtrsim m^{1/3}\Delta^{2/3}$ with m being either m_u or m_d . In particular, the electron contribution to the thermodynamic potential in the CFL phase favours the K^0 condensation (the CFL- K^0 phase) [200, 201, 202, 203]. The phase structure with the CFL- K^0 state and its variants have been also investigated in the NJL-type model [204, 205]. The onset of the K^0 condensation depends on the strength of the $U(1)_A$ anomaly χ as is evident from (70).

In view of (70) the meson masses have the ordering $M_{\pi^\pm} > M_{K^\pm} \simeq M_{K^0}$ for $m_s \gg m_u \approx m_d$ and $\chi \approx 0$, which is inverse of the ordinary ordering in the vacuum [198]. This is, however, natural from the diquark picture as already implied by the order parameter (14) in which CFL- σ meson consists of two diquarks, $\bar{q}\bar{q}qq$. The Nambu-Goldstone bosons are accordingly composed from $\bar{q}\bar{q}qq$; CFL- π^+ contains a $\bar{d}\bar{s}$ diquark that transforms like u quark and an su diquark like \bar{d} quark, while CFL- K^+ a $\bar{d}\bar{s}$ diquark and a ud diquark like \bar{s} quark. Therefore CFL- K^+ has a d quark instead of an s quark as compared to CFL- π^+ and thus it becomes lighter than CFL- π^+ . The effect of $\chi \neq 0$ in (70), on the other hand, favours the standard ordering. This is because χ arises from the instanton interaction and induces a mixture of $\bar{q}\bar{q}qq$ and $\bar{q}q$, which is embodied in the $\Delta^2\sigma$ term in (68). If the quark-hadron continuity is realized, not only the pseudo-scalar mesons but also the vector mesons and fermions would obey the spectral continuity. For example, the continuity of flavour-octet vector mesons at low density and the colour-octet gluons at high density together with the fate of the flavour-singlet vector meson have been investigated in the in-medium QCD sum rules [206].

In order to clarify the existence of another critical point associated with the quark-hadron continuity and the formation of K^0 condensation in the CFL phase, it

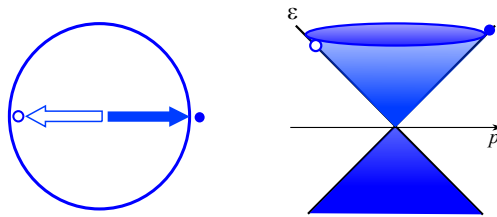


Figure 11. Particle-hole pair near the Fermi surface generating an inhomogeneous chiral condensate with a net momentum, the magnitude of which is given by $2\mu_q$.

is demanded as a theory task to quantify how much the $U(1)_A$ symmetry is effectively restored at finite T and/or μ_q .

7. Inhomogeneous states

In the intermediate density regions of the QCD phase diagram, the ground state may have inhomogeneity with respect to the condensates. The conventional π^- and π^0 condensations induced by the p -wave pion-nucleon interaction in nuclear matter and in neutron matter are well-known examples [207]. In this section, we will address some of the proposed inhomogeneous phases associated with chiral transition and with colour superconductivity.

7.1. Chiral-density waves

In various materials typically at low dimensions, the charge-density wave (CDW) [208] and the spin-density wave (SDW) [209] are realized as ground states. Their counterpart in quark matter is the chiral-density waves: Such a possibility has been discussed in the large N_c limit of QCD [210, 211] with a spatially modulated chiral condensate,

$$\langle \bar{\psi}(x)\psi(x) \rangle = \sigma \cos(2\mathbf{q} \cdot \mathbf{x}), \quad (71)$$

with $|\mathbf{q}| = \mu_q$. Figure 11 is a schematic picture of the pairing of a quark and a quark-hole which makes an inhomogeneous condensate. The magnitude of the net momentum is given by $2\mu_q$. This pairing is favoured by the forward scattering with singular interaction $\sim 1/q^2$ at high density. The conclusion of [211] is that this chiral-density wave state can be realized only for $N_c \gtrsim 1000N_f$. The reason why large N_c is required is that the gluon interaction $\sim 1/q^2$ is IR screened (Thomas-Fermi screening and Landau damping) by the quark loops of $O(1/N_c)$.

In [212] a different ansatz in 2-flavour case has been investigated;

$$\langle \bar{\psi}(x)\psi(x) \rangle - i\langle \bar{\psi}(x)i\gamma^5\tau_3\psi(x) \rangle = \sigma e^{2i\mathbf{q} \cdot \mathbf{x}}. \quad (72)$$

Here τ_3 is a third component of the flavour Pauli matrices. This type of condensate is known to be realized as the *chiral spiral* in $(1+1)$ -dimensional chiral models at finite density [213]. Recently the chiral spiral in QCD is analyzed with confinement effects taken into account [214]. The confining interaction $\sim 1/(\mathbf{q}^2)^2$ is more IR singular than the perturbative interaction, so that the pairing like drawn in figure 11 may be realized for smaller N_c than discussed in [211].

In addition to the IR singular forward scattering, there is another source to produce a spatial modulation of the chiral condensate. To see this, the Ginzburg-Landau approach is again useful. The general terms of the free energy up to the sixth order including derivatives are [215]

$$\Omega = c_2 M^2 + c_4 M^4 + c'_4 (\nabla M)^2 + c_6 M^6 + c'_6 (\nabla M)^2 M^2 + c''_6 (\Delta M)^2, \quad (73)$$

where M is an order parameter for the chiral phase transition (either the chiral condensate or the constituent quark mass in the chiral limit). Note that the magnitude of M and its spatial variation are assumed to be the same order. If c'_4 is negative, inhomogeneous M tends to be favoured. However, the sign of c'_4 cannot be determined by symmetry argument alone. In the mean-field treatment of the 2-flavour NJL model, the expansion turns out to be

$$\Omega = \frac{\alpha_2}{2} M^2 + \frac{\alpha_4}{4} [M^4 + (\nabla M)^2] + \frac{\alpha_6}{6} [M^6 + 5(\nabla M)^2 M^2 + \frac{1}{2}(\Delta M)^2], \quad (74)$$

where α_2 , α_4 and α_6 are all calculable within the model. In particular, the sign of α_4 controls whether the inhomogeneous state occurs: If it is negative, the first-order transition is driven and simultaneously a spatial modulation develops. Therefore the first-order phase boundary is naturally surrounded by the inhomogeneous state in the QCD phase diagram as illustrated in figure 1. Essentially the same phenomena takes place in the chiral Gross-Neveu model in $(1+1)$ -dimensions [213].

Importance of inhomogeneous phases in the QCD phase diagram has been revisited recently and physics implications have not been fully unveiled. Especially it is an urgent but unanswered question how the inhomogeneous condensate could affect the region around, if any, the QCD critical point.

7.2. Implications from chromomagnetic instability

A similar inhomogeneity arises not only in the chiral condensate but also in the diquark condensate $\Delta(x)$. The CFL phase is rigid and $\Delta_{ud} \simeq \Delta_{ds} \simeq \Delta_{su} \simeq \Delta$ as long as $\delta\mu_q = m_s^2/\mu_q < 2\Delta$. Once the Fermi surface mismatch $\delta\mu_q$ exceeds this bound, a new form of colour superconductivity appears, which is a counterpart of what is known as the Sarma state in condensed matter physics. The Sarma state is, however, not stable as it is, and it has been argued that a number constraint such as the charge neutrality condition may help the stabilization [216]. In the QCD context [217] such superconducting states are called the gapless 2SC (g2SC) phase [218, 219] and gapless CFL (gCFL) phase [220, 221] in the 2-flavour and 3-flavour cases, respectively.

It has been found, however, that the gapless superconducting states suffer from another instability problem. In [222, 223, 224, 225, 226] the Meissner (magnetic screening) masses in the g2SC and gCFL phases have been calculated and turned out to be imaginary. That is, there appear negative eigenvalues from the mass-squared matrix in colour space,

$$(m_M^2)^{\alpha\beta} = \frac{1}{3} \sum_{i=1}^3 \left. \frac{\partial^2 \Omega[A]}{\partial A_i^\alpha \partial A_i^\beta} \right|_{A=0}, \quad (75)$$

for transverse gluons A_i^α . This fact is commonly referred to as the *chromomagnetic instability*. The physics implication of the chromomagnetic instability can be nicely articulated by using the Ginzburg-Landau description. A gauged kinetic term can be added to the free energy in a form of

$$\Omega[\Delta, A] \sim \Omega_0[\Delta] - \kappa^{ab} [(\partial_i - igA_i)\Delta]^\dagger{}^a [(\partial^i - igA^i)\Delta]^b, \quad (76)$$

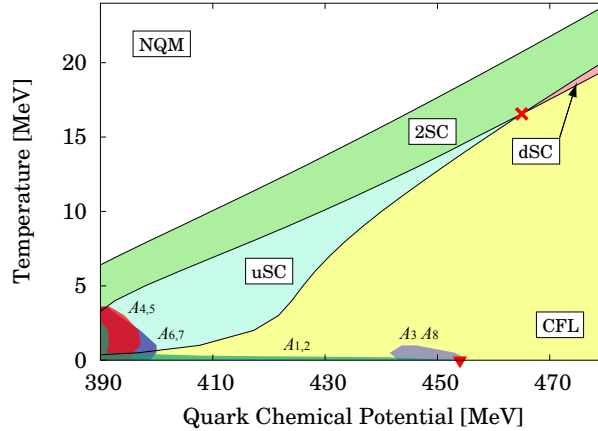


Figure 12. An example of the mean-field model phase diagram with regions suffering from chromomagnetic instability [227]. At high density the ordering is the CFL, dSC and 2SC phases from the bottom to the top as explained in figure 9. At lower density the uSC phase is favoured because the Fermi surface mismatch between d and s quarks is the largest and Δ_{ds} tends to melt first when the critical T is not large. The diagram is drawn with sufficiently large UV cutoff $\Lambda = 1$ GeV and $\Delta \simeq 40$ MeV is chosen at $\mu_q = 500$ MeV, so that the results are robust against cutoff artifacts; otherwise unphysical structures would easily enter.

from which one can derive the Meissner mass-squared as $(m_M^2)^{\alpha\beta} \sim 2\kappa^{ab}(T^\alpha)_{ca}(T^\beta)_{bd}\Delta^c\Delta^d$. We have $\kappa^{33} < 0$ leading to $(m_M^2)^{88} < 0$ in the g2SC phase and also $\kappa^{11} = \kappa^{22} < 0$ leading to $(m_M^2)^{44} - (m_M^2)^{77} < 0$ whose onset is slightly delayed after the gapless onset. The remaining three gluons are unscreened. On the other hand, in the gCFL phase, all eight eigenvalues of the mass-squared matrix can potentially become negative [224, 226, 227]. The unstable regions are mapped out in the NJL model [227] onto the phase diagram, which is presented in figure 12. The shaded regions are unstable with respect to gluons with their colour labelled aside.

Now let us consider a modulation of the diquark condensate in the simplest form of the plane-wave type. This is written as

$$\Delta(x) = |\Delta| e^{iT^\alpha \mathbf{q}^\alpha \cdot \mathbf{x}}, \quad (77)$$

which is known as the (coloured) Fulde-Ferrell-Larkin-Ovchinnikov (FFLO) state [228, 229]. Then, the stability with respect to growth of $\mathbf{q}^\alpha \neq 0$ is deduced from the potential curvature;

$$\frac{1}{3} \sum_{i=3}^3 \frac{\partial \Omega}{\partial q_i^\alpha \partial q_i^\beta} \propto (m_M^2)^{\alpha\beta}. \quad (78)$$

Therefore the chromomagnetic instability leads to the FFLO state. In the g2SC case with $\kappa^{33} < 0$ a non-coloured ($\alpha = 0$) FFLO state may be enough to cure the chromomagnetic instability [230] (see also [231] for results in opposition), but it is a subtle problem if the non-coloured FFLO can stabilize in all colour channels of gluons for 3-flavour quark matter [232].

Generally the instability analysis tells us a tendency towards the destination at best, but cannot go into the ground state. There are several candidates proposed so far, among which the free energy should be compared to sort out the most stable

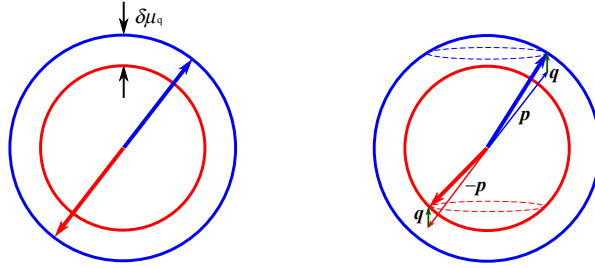


Figure 13. Pairing with a Fermi surface mismatch by $\delta\mu_q$. Left) BCS pairing with vanishing net momentum. One particle is lifted up from the inner Fermi surface by $\delta\mu_q$, which costs an energy. Right) FFLO pairing between particles having momenta $\mathbf{p} + \mathbf{q}$ and $-\mathbf{p} + \mathbf{q}$ with a net momentum $2\mathbf{q}$. The energy costs are reduced around the dotted rings depicted in the figure.

ground state, which is still an open question. Below some of proposals are briefly reviewed.

Crystalline colour superconductivity: It is intuitively understandable that the plane-wave FFLO state is a likely alternative of the ground state if the Fermi surface mismatch grows large. Naturally one can anticipate that $|\mathbf{q}|$ should be of order of $\delta\mu_q$ and actually $|\mathbf{q}| = 1.2\delta\mu_q$ is found in the weak-coupling analysis [62]. The energy gain comes from the ring regions on the Fermi surface as indicated in figure 13. Thus, it is likely that a superposition of multiple \mathbf{q} 's could further decrease the energy by covering the Fermi surface with rings. The general ansatz is then,

$$\langle u(x)d(x) \rangle \sim \Delta_{ud} \sum_{\mathbf{q}_3^a \in \{\mathbf{q}_3\}} e^{2i\mathbf{q}_3^a \cdot \mathbf{x}} \quad (79)$$

for two flavours and, in addition to this, two more condensates,

$$\langle s(x)u(x) \rangle \sim \Delta_{su} \sum_{\mathbf{q}_2^a \in \{\mathbf{q}_2\}} e^{2i\mathbf{q}_2^a \cdot \mathbf{x}}, \quad \langle d(x)s(x) \rangle \sim \Delta_{ds} \sum_{\mathbf{q}_1^a \in \{\mathbf{q}_1\}} e^{2i\mathbf{q}_1^a \cdot \mathbf{x}}, \quad (80)$$

for three flavours [233]. Such a crystal structure has been investigated by means of the Ginzburg-Landau approach [234] with an approximation that $\Delta_{ud} \simeq \Delta_{su}$ and $\langle d(x)s(x) \rangle \simeq 0$ because the Fermi surface mismatch between d , u and s quarks is all the same and the d - s pairing is least favoured (see figure 9). Then, \mathbf{q}_3^a and \mathbf{q}_2^a are optimized so that the free energy becomes smaller. In the 2-flavour case the ground state takes the face-centred-cubic (FCC) structure with eight \mathbf{q}_3^a vectors. In the 3-flavour case, a most stable structure is the 2Cube45z that forms two cubic sets by \mathbf{q}_2^a and \mathbf{q}_3^a with a relative rotation by 45° around the z axis. Another most stable structure is the CubeX where two rectangles by \mathbf{q}_2^a and \mathbf{q}_3^a cross in the X shape to form a cube. It is desirable to study the crystallography in microscopic models: A recent step towards such direction can be seen e.g. in [235].

Gluonic phase: The most straightforward interpretation of the chromomagnetic instability would be the *gluonic phase* [236] in which gauge fields have a finite

expectation value. If only one component of gluons condenses, it is equivalent with the single plane-wave FFLO state. In fact, an ansatz,

$$\mu_8 = \frac{\sqrt{3}}{2}g\langle A_0^8 \rangle, \quad \mu_3 = g\langle A_0^3 \rangle, \quad g\langle A_z^6 \rangle \neq 0, \quad (81)$$

is considered and named the gluonic cylindrical phase in [237]. Because only one spatial gluon condensate is involved, this state can be mapped to a FFLO-type pairing with a coloured phase factor. On the other hand, multi-gluon condensation cannot be transformed into a single plane-wave FFLO state. In the 2-flavour model the free energy of the preferred gluonic phase has turned out to be smaller than that of the FFLO state in a wide parameter region [238]. Such an example is the gluonic colour-spin locked (GCSL) phase that is defined by the following ansatz,

$$\mu_8 = \frac{\sqrt{3}}{2}g\langle A_0^8 \rangle, \quad g\langle A_y^4 \rangle = g\langle A_z^6 \rangle \neq 0, \quad (82)$$

which is free from the chromomagnetic instability [239]. It is then found that these gluonic phases have a smaller free energy than the single plane-wave FFLO state and the unstable g2SC phase. In most regions the GCSL is the most stable apart from the vicinity of the first-order phase transition to normal quark matter where the gluonic cylindrical phase is energetically favoured. It has not been understood, however, how to generalize the description of the gluonic phase to the 3-flavour case. Moreover, an extension of the gluonic condensation with spatial inhomogeneity may further decrease the free energy [240].

Meson supercurrent state: As we have already emphasized, the CFL phase spontaneously breaks chiral symmetry, where low-energy excitations are described by a chiral effective Lagrangian expressed in terms of colour-singlet modes. Then it is possible to formulate the instability by using the chiral effective Lagrangian [241]. The origin of the instability should be common, but it is no longer the “chromomagnetic” instability since gluons do not appear explicitly but all the physical degrees of freedom are Nambu-Goldstone bosons. Then, instead of gluons, one may expect the condensation of vector fields given by mesons, that is, the meson currents. Such a destination of the ground state is called the *meson supercurrent state*. The description looks different at a glance from the chromomagnetic instability and the single plane-wave FFLO state, but the underlying physics must be closely related. An advantage of using the chiral effective Lagrangian is that the inclusion of the K^0 condensate is straightforward, which is complicated in microscopic models. Such an interpretation as the supercurrent generation is also proposed in [242] not relying on the chiral effective Lagrangian but in terms of phase fluctuations around the diquark condensate.

Mixed phase and phase separation: All the states as we have seen so far should compete with a rather conventional possibility, i.e. the mixed phase. Neutrality conditions with respect to gauge charge enforce the Fermi surface mismatch, but these conditions may be relaxed by a formation of a mixture of CSC and NQM regions as discussed in the 2-flavour case in [243].

To clarify the mixed phase structure, however, the precise determination of the surface tension is indispensable. The balance between the surface tension and the Coulomb energy fixes the typical domain size of the mixed phase structure. Naturally,

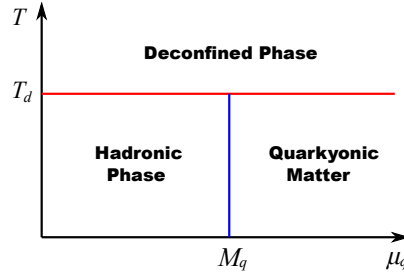


Figure 14. Schematic phase diagram of large- N_c QCD. The pressure is $O(N_c^0)$ in the hadronic phase, $O(N_c)$ in the quarkyonic matter, and $O(N_c^2)$ in the deconfined phase.

the larger the surface tension is, the larger the favoured domain size grows, and eventually the mixed phase should be rather regarded as the phase separation [244]. It is not easy to extract the information on reliable value of the surface tension in the intermediate density region, however. So far, the possibility of the mixed phase in 3-flavour CSC phase has not been studied seriously.

8. Suggestions from QCD-like theories

In the research towards the phase diagram of dense QCD, some knowledge from QCD-like theories would provide us with a useful hint to attack the QCD problem. There are many such attempts and it is impossible to cover all of them in this article. Here, we discuss some selected topics which are highly relevant to the understanding of the dense-QCD phase diagram.

8.1. Quarkyonic matter at large N_c

The novel QCD phase structure in the large N_c limit has been recently proposed [58] as schematically shown in figure 14. When μ_q is smaller than the threshold of the constituent quark mass $M_q \sim M_B/N_c \sim O(N_c^0)$, we have the hadronic phase with zero baryon density at low temperature. As the temperature is increased, there appears the first-order deconfinement transition at $T_d \sim \Lambda_{\text{QCD}}$ at which the number of degrees of freedom and the pressure jump discontinuously from $O(N_c^0)$ to $O(N_c^2)$. Since quark loops are suppressed by $1/N_c$ as compared to gluon contributions, T_d is independent of μ_q in this region as shown in figure 14.

When μ_q becomes greater than M_q , a non-zero baryon density is turned on. The pressure associated with this threshold at $\mu_q \simeq M_q$ changes discontinuously from $O(N_c^0)$ to $O(N_c)$. Also T_d does not change with increasing μ_q as long as $\mu_q \sim O(N_c^0)$, so that quarks are still confined in the right-bottom region ($\mu_q > M_q$ and $T < T_d$) in figure 14. The confining phase with the pressure of $O(N_c)$ is called the *quarkyonic matter* [58].

If we describe the quarkyonic matter as a weakly interacting quark system, the pressure of $O(N_c)$ is a natural consequence, but it is difficult to reconcile it with the confining feature. If we describe the quarkyonic matter as a baryonic system, it must be a strongly interacting matter where the pressure is dominated by baryon interactions of $O(N_c)$ rather than the kinetic pressure of $O(1/N_c)$. A possible idea

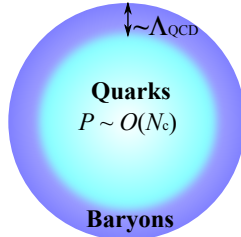


Figure 15. Intuitive picture of the Fermi sphere which accommodates quarkyonic matter — quark Fermi sea and baryonic Fermi surface.

to unify these two descriptions proposed in [58] is illustrated in figure 15; the quarks deep inside the Fermi sphere are weakly interacting, because it is hard to excite these quarks above the Fermi sea due to Pauli blocking. On the other hand, the quarks near the Fermi surface with a shell-width $\sim \Lambda_{\text{QCD}}$ are not affected so much from the Pauli blocking and can interact strongly through IR singular gluons at large N_c . Thus, the bulk thermodynamics such as the pressure, entropy and so on are dominated by the quarks inside the Fermi sphere, while the physical excitations on top of the Fermi surface are dominated by colour-singlet mesons and baryons.

Whether the remnant of quarkyonic matter at large N_c remains in the QCD phase diagram at $N_c = 3$ is an open question. Also, how the chiral transition takes place inside quarkyonic matter is an important problem to be studied. An interesting and plausible possibility comes from the fact that the gluon propagator may be non-perturbative and IR singular because of the confining nature. If this is the case, such IR singular interaction would induce an inhomogeneous chiral condensate as elucidated in section 7.1 or the quarkyonic chiral spiral [214].

8.2. QCD at $N_c = 2$

A QCD-like theory with $N_c = 2$ [245, 246] is also an interesting limit opposite to the case of quarkyonic matter; small N_c instead of large N_c . Two-colour QCD is free from the sign problem if the number of degenerate flavours is even, so that Monte-Carlo simulation at finite baryon density is possible [247]. Two-colour QCD shares many non-perturbative features with $N_c = 3$ QCD such as confinement, chiral symmetry breaking and superfluidity.

In two-colour QCD, baryons consist of quark pairs qq which are bosons. Therefore, nuclear matter composed of fermionic baryons in $N_c = 3$ is replaced by a superfluid state of bosonic baryons in $N_c = 2$. The order parameter of superfluidity is the colour-singlet baryon condensate $\langle qq \rangle$. To investigate the phase structure of two-colour QCD, such baryon condensate has been computed both in numerical simulations and in analytical strong-coupling expansion [248, 249, 250]. There is also a suggestive result that supports the idea of quarkyonic matter in $N_c = 2$ from lattice simulations [251], which is consistent with the model analysis [252]. The correlation functions and excitation spectra can be studied both analytically and numerically for $N_c = 2$. In particular, the low-energy chiral Lagrangian at finite baryon density as well as Leutwyler-Smilga type spectral sum rules have been derived [253]. In-medium hadron spectra as a function of the baryon chemical potential have been also investigated [254, 255, 256]. As can be seen in these examples, two-colour QCD continues to be a

cold atoms	dense QCD
b (bosonic atom)	D (spin-0 diquark)
$f_{\uparrow,\downarrow}$ (fermionic atom)	$q_{\uparrow,\downarrow}$ (unpaired quark)
$N_{\uparrow,\downarrow}$ (b-f molecule)	$\mathcal{N}_{\uparrow,\downarrow}$ (D - q bound state = nucleon)
b-f attraction	gluonic D - q attraction
b-BEC	2SC
N-BCS	nucleon superfluidity

Table 4. Correspondence between the boson-fermion mixture in ultracold atoms (such as ^{87}Rb and ^{40}K mixture) and the diquark-quark mixture in 2-flavour QCD.

valuable testing ground for studying hot/dense QCD at $N_c = 3$.

8.3. Ultracold atoms

High density QCD matter and ultracold atomic systems, although differing by some twenty orders of magnitude in energy scales, share analogous physical aspects [257]. Phenomenological studies of QCD indicate a strong spin-singlet diquark correlation inside the nucleon [258]. Therefore, it may be a good starting point to model the transition from 2-flavour quark matter at high density to nuclear matter at low density in terms of a boson-fermion mixture, in which small-size diquarks are the bosons, unpaired quarks the fermions and the extended nucleons are regarded as composite Bose-Fermi particles [259].

Recent advances in atomic physics have made it possible indeed to realize a boson-fermion mixture in the laboratory. In particular, tuning the atomic interaction via a Feshbach resonance allows formation of heteronuclear molecules, as recently observed in a mixture of ^{87}Rb and ^{40}K atomic vapours in an optical dipole trap [260]. An analysis of such non-relativistic mixture of cold atoms indicate that the BCS-like superfluidity of composite fermion ($N=b+f$) with a small gap is a natural consequence of the strong boson-fermion attraction [259], which may explain the reason why the fermion gap in nucleon superfluidity can be an order of magnitude smaller than the gap in colour superconductivity. A possible correspondence between cold atoms and QCD is summarized in table 4. Fuller understanding, both theoretical and experimental, of the boson-fermion mixture as well as a mixture of three species of atomic fermions [261, 262] may further reveal properties of high-density QCD.

9. Summary and concluding remarks

In this article we reviewed the current status of theoretical investigations to explore the QCD phase structure at finite temperature (T) and finite baryon chemical potential (μ_B). There are (at least) three fundamental states of matter in QCD: the hadronic matter with broken chiral symmetry and quark confinement in the low- T and low- μ_B region, the quark-gluon plasma at high T and the colour superconductivity at low T and high μ_B . On top of these states, some exotic phenomena have been conjectured, e.g. the chiral-density waves, the crystalline colour superconductivity, the gluonic phase, the quakyonic matter and the quark-hadron continuity, as covered in this article, and even more possibilities are still developing. Lattice QCD simulations, the Ginzburg-Landau-Wilson approach and effective theories of QCD are useful theoretical

tools to study these phenomena.

From the experimental point of view, the QCD phase transitions at high T with $\mu_B/T < 1$ can be studied by using high-energy heavy-ion collisions at RHIC and LHC. The QCD phase diagram at relatively low T with $\mu_B/T \gtrsim 1$ may also be probed in the future facilities with lower-energy heavy-ion beams. Besides, recent attempts to determine the mass and the radius of neutron stars from X-ray bursts would be an alternative way to access the equation of state of dense QCD [263, 264]. Furthermore, gravitational waves [265] and neutrinos from supernova explosions [266] or cooling processes in the neutron star [267] carry valuable information of dense QCD matter. Dense QCD shall continue to be one of the most fascinating theoretical and experimental topics in particle, nuclear and astro physics.

K. F. was supported by Japanese MEXT grant (No. 20740134) and also supported in part by Yukawa International Program for Quark Hadron Sciences. T. H. was supported in part by the Grant-in-Aid for Scientific Research on Innovative Areas (No. 2004: 20105003) and by Japanese MEXT grant (No. 22340052).

References

- [1] Y. Nambu, “A systematics of hadrons in subnuclear physics,” *Preludes In Theoretical Physics* (1966) 133–142.
- [2] H. D. Politzer, “Reliable perturbative results for strong interactions?,” *Phys. Rev. Lett.* **30** (1973) 1346–1349.
- [3] D. J. Gross and F. Wilczek, “Ultraviolet behavior of non-abelian gauge theories,” *Phys. Rev. Lett.* **30** (1973) 1343–1346.
- [4] P. Stankus, (ed.), D. Silvermyr, (ed.), S. Sorensen, (ed.), and V. Greene, (ed.), “Ultrarelativistic nucleus nucleus collisions. Proceedings, 21st International Conference, Quark matter, Knoxville, USA, March 30-April 4, 2009,” *Nucl. Phys.* **A830** (2009) 1c–968c.
- [5] N. Armesto, (ed.) *et al.*, “Heavy Ion Collisions at the LHC - Last Call for Predictions,” *J. Phys.* **G35** (2008) 054001, [arXiv:0711.0974 \[hep-ph\]](#).
- [6] H. Heiselberg and M. Hjorth-Jensen, “Phases of dense matter in neutron stars,” *Phys. Rept.* **328** (2000) 237–327, [arXiv:nucl-th/9902033](#).
- [7] D. J. Gross, R. D. Pisarski, and L. G. Yaffe, “QCD and instantons at finite temperature,” *Rev. Mod. Phys.* **53** (1981) 43.
- [8] B. Svetitsky, “Symmetry aspects of finite temperature confinement transitions,” *Phys. Rept.* **132** (1986) 1–53.
- [9] S. P. Klevansky, “The Nambu-Jona-Lasinio model of quantum chromodynamics,” *Rev. Mod. Phys.* **64** (1992) 649–708.
- [10] T. Hatsuda and T. Kunihiro, “QCD phenomenology based on a chiral effective Lagrangian,” *Phys. Rept.* **247** (1994) 221–367, [arXiv:hep-ph/9401310](#).
- [11] H. Meyer-Ortmanns, “Phase transitions in quantum chromodynamics,” *Rev. Mod. Phys.* **68** (1996) 473–598, [arXiv:hep-lat/9608098](#).
- [12] A. V. Smilga, “Physics of thermal QCD,” *Phys. Rept.* **291** (1997) 1–106, [arXiv:hep-ph/9612347](#).
- [13] K. Rajagopal and F. Wilczek, “The condensed matter physics of QCD,” [arXiv:hep-ph/0011333](#).
- [14] D. H. Rischke, “The quark-gluon plasma in equilibrium,” *Prog. Part. Nucl. Phys.* **52** (2004) 197–296, [arXiv:nucl-th/0305030](#).
- [15] M. G. Alford, A. Schmitt, K. Rajagopal, and T. Schafer, “Color superconductivity in dense quark matter,” *Rev. Mod. Phys.* **80** (2008) 1455–1515, [arXiv:0709.4635 \[hep-ph\]](#).
- [16] R. S. Hayano and T. Hatsuda, “Hadron properties in the nuclear medium,” [arXiv:0812.1702 \[nucl-ex\]](#).
- [17] H. Satz, “The states of matter in QCD,” [arXiv:0903.2778 \[hep-ph\]](#).

- [18] M. Huang, “QCD phase diagram at high temperature and density,” [arXiv:1001.3216 \[hep-ph\]](#).
- [19] A. Schmitt, “Dense matter in compact stars - A pedagogical introduction,” [arXiv:1001.3294 \[astro-ph.SR\]](#).
- [20] N. Cabibbo and G. Parisi, “Exponential hadronic spectrum and quark liberation,” *Phys. Lett.* **B59** (1975) 67–69.
- [21] R. Hagedorn, “Statistical thermodynamics of strong interactions at high-energies,” *Nuovo Cim. Suppl.* **3** (1965) 147–186.
- [22] J. C. Collins and M. J. Perry, “Superdense matter: neutrons or asymptotically free quarks?,” *Phys. Rev. Lett.* **34** (1975) 1353.
- [23] G. Baym, “RHIC: From dreams to beams in two decades,” *Nucl. Phys.* **A698** (2002) XXIII–XXXII, [arXiv:hep-ph/0104138](#).
- [24] K. Fukushima, “Chiral symmetry and heavy-ion collisions,” *J. Phys.* **G35** (2008) 104020, [arXiv:0806.0292 \[hep-ph\]](#).
- [25] R. Hagedorn, “How we got to QCD matter from the hadron side by trial and error,” *Lect. Notes Phys.* **221** (1985) 53–76.
- [26] G. Baym, “Confinement of quarks in nuclear matter,” *Physica* **96A** (1979) 131–135.
- [27] H. Satz, “Deconfinement and percolation,” *Nucl. Phys.* **A642** (1998) 130–142, [arXiv:hep-ph/9805418](#).
- [28] T. Hatsuda and T. Kunihiro, “Fluctuation effects in hot quark matter: precursors of chiral transition at finite temperature,” *Phys. Rev. Lett.* **55** (1985) 158–161.
- [29] P. Gerber and H. Leutwyler, “Hadrons below the chiral phase transition,” *Nucl. Phys.* **B321** (1989) 387.
- [30] E. G. Drukarev and E. M. Levin, “Structure of nuclear matter and QCD sum rules,” *Prog. Part. Nucl. Phys.* **27** (1991) 77–134.
- [31] T. D. Cohen, R. J. Furnstahl, and D. K. Griegel, “Quark and gluon condensates in nuclear matter,” *Phys. Rev.* **C45** (1992) 1881–1893.
- [32] T. Hatsuda and S. H. Lee, “QCD sum rules for vector mesons in nuclear medium,” *Phys. Rev.* **C46** (1992) 34–38.
- [33] N. Kaiser, P. de Homont, and W. Weise, “In-medium chiral condensate beyond linear density approximation,” *Phys. Rev.* **C77** (2008) 025204, [arXiv:0711.3154 \[nucl-th\]](#).
- [34] N. Kaiser and W. Weise, “Chiral condensate in neutron matter,” *Phys. Lett.* **B671** (2009) 25–29, [arXiv:0808.0856 \[nucl-th\]](#).
- [35] B. Svetitsky and L. G. Yaffe, “Critical behavior at finite temperature confinement transitions,” *Nucl. Phys.* **B210** (1982) 423.
- [36] R. D. Pisarski and F. Wilczek, “Remarks on the chiral phase transition in chromodynamics,” *Phys. Rev.* **D29** (1984) 338–341.
- [37] M. Fukugita, M. Okawa, and A. Ukawa, “Finite size scaling study of the deconfining phase transition in pure SU(3) lattice gauge theory,” *Nucl. Phys.* **B337** (1990) 181.
- [38] Y. Aoki, G. Endrodi, Z. Fodor, S. D. Katz, and K. K. Szabo, “The order of the quantum chromodynamics transition predicted by the standard model of particle physics,” *Nature* **443** (2006) 675–678, [arXiv:hep-lat/0611014](#).
- [39] C. DeTar and U. M. Heller, “QCD thermodynamics from the lattice,” *Eur. Phys. J.* **A41** (2009) 405–437, [arXiv:0905.2949 \[hep-lat\]](#).
- [40] C. E. DeTar, “A conjecture concerning the modes of excitation of the quark-gluon plasma,” *Phys. Rev.* **D32** (1985) 276.
- [41] M. Kitazawa, T. Koide, T. Kunihiro, and Y. Nemoto, “Precursor of color superconductivity in hot quark matter,” *Phys. Rev.* **D65** (2002) 091504, [arXiv:nucl-th/0111022](#).
- [42] H. Abuki, T. Hatsuda, and K. Itakura, “Structural change of Cooper pairs and momentum-dependent gap in color superconductivity,” *Phys. Rev.* **D65** (2002) 074014, [arXiv:hep-ph/0109013](#).
- [43] Y. Nishida and H. Abuki, “BCS-BEC crossover in relativistic superfluid and its possible realization in QCD,” *Phys. Rev.* **D72** (2005) 096004, [arXiv:hep-ph/0504083](#).
- [44] Q. Chena, J. Stajicb, S. Tan, and K. Levin, “BCS-BEC crossover: From high temperature superconductors to ultracold superfluids,” *Phys. Rep.* **412** (2005) 1.
- [45] M. Asakawa and K. Yazaki, “Chiral restoration at finite density and temperature,” *Nucl. Phys.* **A504** (1989) 668–684.
- [46] A. Barducci, R. Casalbuoni, S. De Curtis, R. Gatto, and G. Pettini, “Chiral symmetry breaking in QCD at finite temperature and density,” *Phys. Lett.* **B231** (1989) 463.
- [47] F. Wilczek, “Application of the renormalization group to a second order QCD phase transition,” *Int. J. Mod. Phys.* **A7** (1992) 3911–3925.

- [48] J. Berges and K. Rajagopal, “Color superconductivity and chiral symmetry restoration at nonzero baryon density and temperature,” *Nucl. Phys.* **B538** (1999) 215–232, [arXiv:hep-ph/9804233](#).
- [49] M. A. Stephanov, K. Rajagopal, and E. V. Shuryak, “Signatures of the tricritical point in QCD,” *Phys. Rev. Lett.* **81** (1998) 4816–4819, [arXiv:hep-ph/9806219](#).
- [50] M. A. Stephanov, K. Rajagopal, and E. V. Shuryak, “Event-by-event fluctuations in heavy ion collisions and the QCD critical point,” *Phys. Rev.* **D60** (1999) 114028, [arXiv:hep-ph/9903292](#).
- [51] P. Chomaz, “The nuclear liquid gas phase transition and phase coexistence: A review,” [arXiv:nucl-ex/0410024](#).
- [52] J. Cleymans, H. Oeschler, and K. Redlich, “Influence of impact parameter on thermal description of relativistic heavy ion collisions at (1-2) A-GeV,” *Phys. Rev.* **C59** (1999) 1663, [arXiv:nucl-th/9809027](#).
- [53] F. Becattini, J. Manninen, and M. Gazdzicki, “Energy and system size dependence of chemical freeze-out in relativistic nuclear collisions,” *Phys. Rev.* **C73** (2006) 044905, [arXiv:hep-ph/0511092](#).
- [54] A. Andronic, P. Braun-Munzinger, and J. Stachel, “Thermal hadron production in relativistic nuclear collisions: the sigma meson, the horn, and the QCD phase transition,” *Phys. Lett.* **B673** (2009) 142, [arXiv:0812.1186 \[nucl-th\]](#).
- [55] P. Braun-Munzinger, J. Stachel, and C. Wetterich, “Chemical freeze-out and the QCD phase transition temperature,” *Phys. Lett.* **B596** (2004) 61–69, [arXiv:nucl-th/0311005](#).
- [56] G. ’t Hooft, “A planar diagram theory for strong interactions,” *Nucl. Phys.* **B72** (1974) 461.
- [57] E. Witten, “Baryons in the $1/n$ expansion,” *Nucl. Phys.* **B160** (1979) 57.
- [58] L. McLerran and R. D. Pisarski, “Phases of cold, dense quarks at large N_c ,” *Nucl. Phys.* **A796** (2007) 83–100, [arXiv:0706.2191 \[hep-ph\]](#).
- [59] A. Andronic *et al.*, “Hadron production in ultra-relativistic nuclear collisions: Quarkyonic matter and a triple point in the phase diagram of QCD,” *Nucl. Phys.* **A837** (2010) 65–86, [arXiv:0911.4806 \[hep-ph\]](#).
- [60] B. C. Barrois, “Superconducting quark matter,” *Nucl. Phys.* **B129** (1977) 390.
- [61] D. Bailin and A. Love, “Superfluidity and superconductivity in relativistic fermion systems,” *Phys. Rept.* **107** (1984) 325.
- [62] M. G. Alford, J. A. Bowers, and K. Rajagopal, “Crystalline color superconductivity,” *Phys. Rev.* **D63** (2001) 074016, [arXiv:hep-ph/0008208](#).
- [63] A. M. Polyakov, “Thermal properties of gauge fields and quark liberation,” *Phys. Lett.* **B72** (1978) 477–480.
- [64] L. Susskind, “Lattice models of quark confinement at high temperature,” *Phys. Rev.* **D20** (1979) 2610–2618.
- [65] L. D. McLerran and B. Svetitsky, “Quark liberation at high temperature: A Monte Carlo study of SU(2) gauge theory,” *Phys. Rev.* **D24** (1981) 450.
- [66] S. Nadkarni, “Nonabelian Debye screening. 1. The color averaged potential,” *Phys. Rev.* **D33** (1986) 3738.
- [67] S. Nadkarni, “Nonabelian Debye screening. 2. The singlet potential,” *Phys. Rev.* **D34** (1986) 3904.
- [68] P. B. Arnold and L. G. Yaffe, “The non-Abelian Debye screening length beyond leading order,” *Phys. Rev.* **D52** (1995) 7208–7219, [arXiv:hep-ph/9508280](#).
- [69] A. Hart, M. Laine, and O. Philipsen, “Static correlation lengths in QCD at high temperatures and finite densities,” *Nucl. Phys.* **B586** (2000) 443–474, [arXiv:hep-ph/0004060](#).
- [70] **WHOT-QCD** Collaboration, Y. Maezawa *et al.*, “Electric and magnetic screening masses at finite temperature from generalized Polyakov-line correlations in two-flavor lattice QCD,” [arXiv:1003.1361 \[hep-lat\]](#).
- [71] M. Ogilvie, “An effective spin model for finite temperature QCD,” *Phys. Rev. Lett.* **52** (1984) 1369.
- [72] M. Okawa, “Universality of deconfining phase transition in (3+1)-dimensional SU(2) lattice gauge theory,” *Phys. Rev. Lett.* **60** (1988) 1805.
- [73] F. Karsch and S. Stickan, “The three-dimensional, three-state Potts model in an external field,” *Phys. Lett.* **B488** (2000) 319–325, [arXiv:hep-lat/0007019](#).
- [74] B. Lucini, M. Teper, and U. Wenger, “The high temperature phase transition in SU(N) gauge theories,” *JHEP* **01** (2004) 061, [arXiv:hep-lat/0307017](#).
- [75] S. Datta and S. Gupta, “Scaling and the continuum limit of the finite temperature deconfinement transition in SU(N_c) pure gauge theory,” *Phys. Rev.* **D80** (2009) 114504, [arXiv:0909.5591 \[hep-lat\]](#).

- [76] F. Y. Wu, “The Potts model,” *Rev. Mod. Phys.* **54** (1982) 235–268.
- [77] C. E. DeTar and L. D. McLerran, “Order parameters for the confinement - deconfinement phase transition in $SU(N)$ gauge theories with quarks,” *Phys. Lett.* **B119** (1982) 171.
- [78] C. Gattringer, “Linking confinement to spectral properties of the Dirac operator,” *Phys. Rev. Lett.* **97** (2006) 032003, [arXiv:hep-lat/0605018](#).
- [79] E. Bilgici, F. Bruckmann, C. Gattringer, and C. Hagen, “Dual quark condensate and dressed Polyakov loops,” *Phys. Rev.* **D77** (2008) 094007, [arXiv:0801.4051 \[hep-lat\]](#).
- [80] C. S. Fischer, “Deconfinement phase transition and the quark condensate,” *Phys. Rev. Lett.* **103** (2009) 052003, [arXiv:0904.2700 \[hep-ph\]](#).
- [81] R. V. Gavai, A. Gocksch, and M. Ogilvie, “The effective action in Monte Carlo calculations with dynamical fermions,” *Phys. Rev. Lett.* **56** (1986) 815.
- [82] A. P. Balachandran, S. Digal, and T. Matsuura, “Semi-superfluid strings in high density QCD,” *Phys. Rev.* **D73** (2006) 074009, [arXiv:hep-ph/0509276](#).
- [83] E. V. Shuryak, “Which chiral symmetry is restored in hot QCD?,” *Comments Nucl. Part. Phys.* **21** (1994) 235–248, [arXiv:hep-ph/9310253](#).
- [84] J. Stern, “Two alternatives of spontaneous chiral symmetry breaking in QCD,” [arXiv:hep-ph/9801282](#).
- [85] I. I. Kogan, A. Kovner, and M. A. Shifman, “Chiral symmetry breaking without bilinear condensates, unbroken axial $Z(N)$ symmetry, and exact QCD inequalities,” *Phys. Rev.* **D59** (1999) 016001, [arXiv:hep-ph/9807286](#).
- [86] Y. Watanabe, K. Fukushima, and T. Hatsuda, “Order parameters with higher dimensionful composite fields,” *Prog. Theor. Phys.* **111** (2004) 967–972, [arXiv:hep-th/0312271](#).
- [87] M. Harada, C. Sasaki, and S. Takemoto, “Enhancement of quark number susceptibility with an alternative pattern of chiral symmetry breaking in dense matter,” [arXiv:0908.1361 \[hep-ph\]](#).
- [88] M. G. Alford, K. Rajagopal, and F. Wilczek, “Color-flavor locking and chiral symmetry breaking in high density QCD,” *Nucl. Phys.* **B537** (1999) 443–458, [arXiv:hep-ph/9804403](#).
- [89] M. Kobayashi and T. Maskawa, “Chiral symmetry and eta-x mixing,” *Prog. Theor. Phys.* **44** (1970) 1422–1424.
- [90] M. Kobayashi, H. Kondo, and T. Maskawa, “Symmetry breaking of the chiral $u(3) \times u(3)$ and the quark model,” *Prog. Theor. Phys.* **45** (1971) 1955–1959.
- [91] G. ’t Hooft, “Symmetry breaking through Bell-Jackiw anomalies,” *Phys. Rev. Lett.* **37** (1976) 8–11.
- [92] G. ’t Hooft, “Computation of the quantum effects due to a four- dimensional pseudoparticle,” *Phys. Rev.* **D14** (1976) 3432–3450.
- [93] **Particle Data Group** Collaboration, C. Amsler *et al.*, “Review of particle physics,” *Phys. Lett.* **B667** (2008) 1.
- [94] F. R. Brown *et al.*, “On the existence of a phase transition for QCD with three light quarks,” *Phys. Rev. Lett.* **65** (1990) 2491–2494.
- [95] S. Gavin, A. Gocksch, and R. D. Pisarski, “QCD and the chiral critical point,” *Phys. Rev.* **D49** (1994) 3079–3082, [arXiv:hep-ph/9311350](#).
- [96] Y. Hatta and T. Ikeda, “Universality, the QCD critical / tricritical point and the quark number susceptibility,” *Phys. Rev.* **D67** (2003) 014028, [arXiv:hep-ph/0210284](#).
- [97] E. K. Riedel and F. J. Wegner, “Tricritical exponents and scaling fields,” *Phys. Rev. Lett.* **29** (1972) 349–352.
- [98] B.-J. Schaefer and J. Wambach, “Susceptibilities near the QCD (tri)critical point,” *Phys. Rev.* **D75** (2007) 085015, [arXiv:hep-ph/0603256](#).
- [99] **MILC** Collaboration, C. Bernard *et al.*, “QCD thermodynamics with three flavors of improved staggered quarks,” *Phys. Rev.* **D71** (2005) 034504, [arXiv:hep-lat/0405029](#).
- [100] M. Cheng *et al.*, “The transition temperature in QCD,” *Phys. Rev.* **D74** (2006) 054507, [arXiv:hep-lat/0608013](#).
- [101] Y. Aoki, Z. Fodor, S. D. Katz, and K. K. Szabo, “The QCD transition temperature: Results with physical masses in the continuum limit,” *Phys. Lett.* **B643** (2006) 46–54, [arXiv:hep-lat/0609068](#).
- [102] Y. Maezawa *et al.*, “Thermodynamics of two-flavor lattice QCD with an improved Wilson quark action at non-zero temperature and density,” *J. Phys.* **G34** (2007) S651–654, [arXiv:hep-lat/0702005](#).
- [103] Y. Aoki *et al.*, “The QCD transition temperature: results with physical masses in the continuum limit II,” *JHEP* **06** (2009) 088, [arXiv:0903.4155 \[hep-lat\]](#).
- [104] A. Bazavov *et al.*, “Equation of state and QCD transition at finite temperature,” *Phys. Rev.* **D80** (2009) 014504, [arXiv:0903.4379 \[hep-lat\]](#).

- [105] V. G. Bornyakov *et al.*, “Probing the finite temperature phase transition with $N_f = 2$ nonperturbatively improved Wilson fermions,” [arXiv:0910.2392 \[hep-lat\]](#).
- [106] M. Cheng *et al.*, “The finite temperature QCD using 2+1 flavors of domain wall fermions at $N_t = 8$,” [arXiv:0911.3450 \[hep-lat\]](#).
- [107] **Wuppertal-Budapest** Collaboration, S. Borsanyi *et al.*, “Is there still any T_c mystery in lattice QCD? Results with physical masses in the continuum limit III,” [arXiv:1005.3508 \[hep-lat\]](#).
- [108] **HotQCD** Collaboration, A. Bazavov and P. Petreczky, “Deconfinement and chiral transition with the highly improved staggered quark (HISQ) action,” *J. Phys. Conf. Ser.* **230** (2010) 012014, [arXiv:1005.1131 \[hep-lat\]](#).
- [109] S. Muroya, A. Nakamura, C. Nonaka, and T. Takaishi, “Lattice QCD at finite density: An introductory review,” *Prog. Theor. Phys.* **110** (2003) 615–668, [arXiv:hep-lat/0306031](#).
- [110] S. Ejiri, “Recent progress in lattice QCD at finite density,” *PoS LATTICE2008* (2008) 002, [arXiv:0812.1534 \[hep-lat\]](#).
- [111] M. P. Lombardo, K. Splittorff, and J. J. M. Verbaarschot, “Lattice QCD and dense quark matter,” [arXiv:0912.4410 \[hep-lat\]](#).
- [112] **UKQCD** Collaboration, I. M. Barbour, “Problems in simulating QCD at finite density on a lattice,” *Nucl. Phys.* **A642** (1998) 251–262.
- [113] Z. Fodor and S. D. Katz, “Lattice determination of the critical point of QCD at finite T and μ ,” *JHEP* **03** (2002) 014, [arXiv:hep-lat/0106002](#).
- [114] C. R. Allton *et al.*, “The QCD thermal phase transition in the presence of a small chemical potential,” *Phys. Rev.* **D66** (2002) 074507, [arXiv:hep-lat/0204010](#).
- [115] C. R. Allton *et al.*, “Thermodynamics of two flavor QCD to sixth order in quark chemical potential,” *Phys. Rev.* **D71** (2005) 054508, [arXiv:hep-lat/0501030](#).
- [116] R. V. Gavai and S. Gupta, “QCD at finite chemical potential with six time slices,” *Phys. Rev.* **D78** (2008) 114503, [arXiv:0806.2233 \[hep-lat\]](#).
- [117] M. G. Alford, A. Kapustin, and F. Wilczek, “Imaginary chemical potential and finite fermion density on the lattice,” *Phys. Rev.* **D59** (1999) 054502, [arXiv:hep-lat/9807039](#).
- [118] P. de Forcrand and O. Philipsen, “The QCD phase diagram for small densities from imaginary chemical potential,” *Nucl. Phys.* **B642** (2002) 290–306, [arXiv:hep-lat/0205016](#).
- [119] A. Roberge and N. Weiss, “Gauge theories with imaginary chemical potential and the phases of QCD,” *Nucl. Phys.* **B275** (1986) 734.
- [120] Y. Sakai, K. Kashiwa, H. Kouno, and M. Yahiro, “Phase diagram in the imaginary chemical potential region and extended Z_3 symmetry,” *Phys. Rev.* **D78** (2008) 036001, [arXiv:0803.1902 \[hep-ph\]](#).
- [121] D. E. Miller and K. Redlich, “Exact implementation of baryon number conservation in lattice gauge theory,” *Phys. Rev.* **D35** (1987) 2524.
- [122] A. Hasenfratz and D. Toussaint, “Canonical ensembles and nonzero density quantum chromodynamics,” *Nucl. Phys.* **B371** (1992) 539–549.
- [123] J. Engels, O. Kaczmarek, F. Karsch, and E. Laermann, “The quenched limit of lattice QCD at non-zero baryon number,” *Nucl. Phys.* **B558** (1999) 307–326, [arXiv:hep-lat/9903030](#).
- [124] S. Kratochvila and P. de Forcrand, “The canonical approach to finite density QCD,” *PoS LAT2005* (2006) 167, [arXiv:hep-lat/0509143](#).
- [125] A. Li, X. Meng, A. Alexandru, and K.-F. Liu, “Finite density simulations with canonical ensemble,” *PoS LATTICE2008* (2008) 178, [arXiv:0810.2349 \[hep-lat\]](#).
- [126] K. Fukushima, “Thermodynamic limit of the canonical partition function with respect to the quark number in QCD,” *Ann. Phys.* **304** (2003) 72–88, [arXiv:hep-ph/0204302](#).
- [127] A. Gocksch, “Simulating lattice QCD at finite density,” *Phys. Rev. Lett.* **61** (1988) 2054.
- [128] S. Ejiri, “On the existence of the critical point in finite density lattice QCD,” *Phys. Rev.* **D77** (2008) 014508, [arXiv:0706.3549 \[hep-lat\]](#).
- [129] K. N. Anagnostopoulos and J. Nishimura, “New approach to the complex-action problem and its application to a nonperturbative study of superstring theory,” *Phys. Rev.* **D66** (2002) 106008, [arXiv:hep-th/0108041](#).
- [130] J. Ambjorn, K. N. Anagnostopoulos, J. Nishimura, and J. J. M. Verbaarschot, “The factorization method for systems with a complex action -a test in Random Matrix Theory for finite density QCD-,” *JHEP* **10** (2002) 062, [arXiv:hep-lat/0208025](#).
- [131] Z. Fodor, S. D. Katz, and C. Schmidt, “The density of states method at non-zero chemical potential,” *JHEP* **03** (2007) 121, [arXiv:hep-lat/0701022](#).
- [132] D. T. Son and M. A. Stephanov, “QCD at finite isospin density,” *Phys. Rev. Lett.* **86** (2001) 592–595, [arXiv:hep-ph/0005225](#).
- [133] K. Splittorff and J. J. M. Verbaarschot, “The approach to the thermodynamic limit in lattice

- QCD at $\mu \neq 0$,” *Phys. Rev.* **D77** (2008) 014514, [arXiv:0709.2218](#) [[hep-lat](#)].
- [134] M. D’Elia and F. Sanfilippo, “Thermodynamics of two flavor QCD from imaginary chemical potentials,” *Phys. Rev.* **D80** (2009) 014502, [arXiv:0904.1400](#) [[hep-lat](#)].
- [135] M. P. Lombardo, K. Splittorff, and J. J. M. Verbaarschot, “Distributions of the phase angle of the fermion determinant in QCD,” *Phys. Rev.* **D80** (2009) 054509, [arXiv:0904.2122](#) [[hep-lat](#)].
- [136] **WHOT-QCD** Collaboration, S. Ejiri *et al.*, “Equation of state and heavy-quark free energy at finite temperature and density in two flavor lattice QCD with Wilson quark action,” [arXiv:0909.2121](#) [[hep-lat](#)].
- [137] G. Parisi and Y.-s. Wu, “Perturbation theory without gauge fixing,” *Sci. Sin.* **24** (1981) 483.
- [138] G. Parisi, “On complex probabilities,” *Phys. Lett.* **B131** (1983) 393–395.
- [139] J. R. Klauder, “Coherent state Langevin equations for canonical quantum systems with applications to the quantized hall effect,” *Phys. Rev.* **A29** (1984) 2036–2047.
- [140] P. H. Damgaard and H. Huffel, “Stochastic quantization,” *Phys. Rept.* **152** (1987) 227.
- [141] M. Namiki *et al.*, “Stochastic quantization,” *Lect. Notes Phys.* **M9** (1992) 1–217.
- [142] G. Aarts, E. Seiler, and I.-O. Stamatescu, “The complex Langevin method: When can it be trusted?,” *Phys. Rev.* **D81** (2010) 054508, [arXiv:0912.3360](#) [[hep-lat](#)].
- [143] G. Aarts and K. Splittorff, “Degenerate distributions in complex Langevin dynamics: one-dimensional QCD at finite chemical potential,” [arXiv:1006.0332](#) [[hep-lat](#)].
- [144] Z. Fodor and S. D. Katz, “Critical point of QCD at finite T and μ , lattice results for physical quark masses,” *JHEP* **04** (2004) 050, [arXiv:hep-lat/0402006](#).
- [145] S. Ejiri, “Lee-Yang zero analysis for the study of QCD phase structure,” *Phys. Rev.* **D73** (2006) 054502, [arXiv:hep-lat/0506023](#).
- [146] **RBC-Bielefeld** Collaboration, C. Miao and C. Schmidt, “Non-zero density QCD by the Taylor expansion method: The isentropic equation of state, hadronic fluctuations and more,” *PoS LATTICE2008* (2008) 172, [arXiv:0810.0375](#) [[hep-lat](#)].
- [147] J. Wambach, B.-J. Schaefer, and M. Wagner, “QCD thermodynamics: Confronting the Polyakov-quark-meson model with lattice QCD,” [arXiv:0911.0296](#) [[hep-ph](#)].
- [148] S. Ejiri, “Canonical partition function and finite density phase transition in lattice QCD,” *Phys. Rev.* **D78** (2008) 074507, [arXiv:0804.3227](#) [[hep-lat](#)].
- [149] P. de Forcrand and O. Philipsen, “The chiral critical point of $N_f = 3$ QCD at finite density to the order $(\mu/T)^4$,” *JHEP* **11** (2008) 012, [arXiv:0808.1096](#) [[hep-lat](#)].
- [150] P. de Forcrand and O. Philipsen, “The curvature of the critical surface: a progress report,” *PoS LATTICE2008* (2008) 208, [arXiv:0811.3858](#) [[hep-lat](#)].
- [151] T. Schafer and E. V. Shuryak, “Instantons in QCD,” *Rev. Mod. Phys.* **70** (1998) 323–426, [arXiv:hep-ph/9610451](#).
- [152] T. Schafer, “Instanton effects in QCD at high baryon density,” *Phys. Rev.* **D65** (2002) 094033, [arXiv:hep-ph/0201189](#).
- [153] K. Fukushima, “Phase diagrams in the three-flavor Nambu–Jona-Lasinio model with the Polyakov loop,” *Phys. Rev.* **D77** (2008) 114028, [arXiv:0803.3318](#) [[hep-ph](#)].
- [154] K. Fukushima, “Chiral effective model with the Polyakov loop,” *Phys. Lett.* **B591** (2004) 277–284, [arXiv:hep-ph/0310121](#).
- [155] C. Ratti, M. A. Thaler, and W. Weise, “Phases of QCD: Lattice thermodynamics and a field theoretical model,” *Phys. Rev.* **D73** (2006) 014019, [arXiv:hep-ph/0506234](#).
- [156] B.-J. Schaefer, M. Wagner, and J. Wambach, “Thermodynamics of (2+1)-flavor QCD: Confronting models with lattice studies,” *Phys. Rev.* **D81** (2010) 074013, [arXiv:0910.5628](#) [[hep-ph](#)].
- [157] W.-j. Fu, Z. Zhang, and Y.-x. Liu, “2+1 flavor Polyakov–Nambu–Jona-Lasinio model at finite temperature and nonzero chemical potential,” *Phys. Rev.* **D77** (2008) 014006, [arXiv:0711.0154](#) [[hep-ph](#)].
- [158] B.-J. Schaefer and M. Wagner, “The three-flavor chiral phase structure in hot and dense QCD matter,” *Phys. Rev.* **D79** (2009) 014018, [arXiv:0808.1491](#) [[hep-ph](#)].
- [159] J.-W. Chen, K. Fukushima, H. Kohyama, K. Ohnishi, and U. Raha, “ $U_A(1)$ anomaly in hot and dense QCD and the critical surface,” *Phys. Rev.* **D80** (2009) 054012, [arXiv:0901.2407](#) [[hep-ph](#)].
- [160] C. Nonaka and M. Asakawa, “Hydrodynamical evolution near the QCD critical end point,” *Phys. Rev.* **C71** (2005) 044904, [arXiv:nucl-th/0410078](#).
- [161] O. Scavenius, A. Mocsy, I. N. Mishustin, and D. H. Rischke, “Chiral phase transition within effective models with constituent quarks,” *Phys. Rev.* **C64** (2001) 045202, [arXiv:nucl-th/0007030](#).
- [162] H. Fujii, “Scalar density fluctuation at critical end point in NJL model,” *Phys. Rev.* **D67**

- (2003) 094018, [arXiv:hep-ph/0302167](#).
- [163] M. A. Stephanov, “Non-Gaussian fluctuations near the QCD critical point,” *Phys. Rev. Lett.* **102** (2009) 032301, [arXiv:0809.3450 \[hep-ph\]](#).
- [164] D. T. Son and M. A. Stephanov, “Dynamic universality class of the QCD critical point,” *Phys. Rev.* **D70** (2004) 056001, [arXiv:hep-ph/0401052](#).
- [165] H. Fujii and M. Ohtani, “Sigma and hydrodynamic modes along the critical line,” *Phys. Rev.* **D70** (2004) 014016, [arXiv:hep-ph/0402263](#).
- [166] K. Fukushima, “Critical surface in hot and dense QCD with the vector interaction,” *Phys. Rev.* **D78** (2008) 114019, [arXiv:0809.3080 \[hep-ph\]](#).
- [167] S. Klimt, M. Lutz, and W. Weise, “Chiral phase transition in the SU(3) Nambu and Jona-Lasinio model,” *Phys. Lett.* **B249** (1990) 386–390.
- [168] M. Lutz, S. Klimt, and W. Weise, “Meson properties at finite temperature and baryon density,” *Nucl. Phys.* **A542** (1992) 521–558.
- [169] M. Kitazawa, T. Koide, T. Kunihiro, and Y. Nemoto, “Chiral and color superconducting phase transitions with vector interaction in a simple model,” *Prog. Theor. Phys.* **108** (2002) 929–951, [arXiv:hep-ph/0207255](#).
- [170] C. Sasaki, B. Friman, and K. Redlich, “Quark number fluctuations in a chiral model at finite baryon chemical potential,” *Phys. Rev.* **D75** (2007) 054026, [arXiv:hep-ph/0611143](#).
- [171] Y. Sakai, K. Kashiwa, H. Kouno, M. Matsuzaki, and M. Yahiro, “Vector-type four-quark interaction and its impact on QCD phase structure,” *Phys. Rev.* **D78** (2008) 076007, [arXiv:0806.4799 \[hep-ph\]](#).
- [172] M. Iwasaki and T. Iwado, “Superconductivity in the quark matter,” *Phys. Lett.* **B350** (1995) 163–168.
- [173] M. G. Alford, K. Rajagopal, and F. Wilczek, “QCD at finite baryon density: Nucleon droplets and color superconductivity,” *Phys. Lett.* **B422** (1998) 247–256, [arXiv:hep-ph/9711395](#).
- [174] R. Rapp, T. Schafer, E. V. Shuryak, and M. Velkovsky, “Diquark Bose condensates in high density matter and instantons,” *Phys. Rev. Lett.* **81** (1998) 53–56, [arXiv:hep-ph/9711396](#).
- [175] M. G. Alford, J. Berges, and K. Rajagopal, “Unlocking color and flavor in superconducting strange quark matter,” *Nucl. Phys.* **B558** (1999) 219–242, [arXiv:hep-ph/9903502](#).
- [176] S. B. Ruester, I. A. Shovkovy, and D. H. Rischke, “Phase diagram of dense neutral three-flavor quark matter,” *Nucl. Phys.* **A743** (2004) 127–146, [arXiv:hep-ph/0405170](#).
- [177] K. Iida, T. Matsuura, M. Tachibana, and T. Hatsuda, “Melting pattern of diquark condensates in quark matter,” *Phys. Rev. Lett.* **93** (2004) 132001, [arXiv:hep-ph/0312363](#).
- [178] K. Fukushima, C. Kouvaris, and K. Rajagopal, “Heating (gapless) color-flavor locked quark matter,” *Phys. Rev.* **D71** (2005) 034002, [arXiv:hep-ph/0408322](#).
- [179] M. Alford, C. Kouvaris, and K. Rajagopal, “Gapless CFL and its competition with mixed phases,” [arXiv:hep-ph/0407257](#).
- [180] A. Schmitt, Q. Wang, and D. H. Rischke, “When the transition temperature in color superconductors is not like in BCS theory,” *Phys. Rev.* **D66** (2002) 114010, [arXiv:nucl-th/0209050](#).
- [181] A. Schmitt, Q. Wang, and D. H. Rischke, “Electromagnetic Meissner effect in spin-one color superconductors,” *Phys. Rev. Lett.* **91** (2003) 242301, [arXiv:nucl-th/0301090](#).
- [182] A. Schmitt, “The ground state in a spin-one color superconductor,” *Phys. Rev.* **D71** (2005) 054016, [arXiv:nucl-th/0412033](#).
- [183] D. T. Son, “Superconductivity by long-range color magnetic interaction in high-density quark matter,” *Phys. Rev.* **D59** (1999) 094019, [arXiv:hep-ph/9812287](#).
- [184] D. K. Hong, V. A. Miransky, I. A. Shovkovy, and L. C. R. Wijewardhana, “Schwinger-Dyson approach to color superconductivity in dense QCD,” *Phys. Rev.* **D61** (2000) 056001, [arXiv:hep-ph/9906478](#).
- [185] T. Schafer and F. Wilczek, “Superconductivity from perturbative one-gluon exchange in high density quark matter,” *Phys. Rev.* **D60** (1999) 114033, [arXiv:hep-ph/9906512](#).
- [186] R. D. Pisarski and D. H. Rischke, “Color superconductivity in weak coupling,” *Phys. Rev.* **D61** (2000) 074017, [arXiv:nucl-th/9910056](#).
- [187] M. Alford and K. Rajagopal, “Absence of two-flavor color superconductivity in compact stars,” *JHEP* **06** (2002) 031, [arXiv:hep-ph/0204001](#).
- [188] A. W. Steiner, S. Reddy, and M. Prakash, “Color-neutral superconducting quark matter,” *Phys. Rev.* **D66** (2002) 094007, [arXiv:hep-ph/0205201](#).
- [189] A. Gerhold and A. Rebhan, “Gauge dependence identities for color superconducting QCD,” *Phys. Rev.* **D68** (2003) 011502, [arXiv:hep-ph/0305108](#).
- [190] K. Rajagopal and F. Wilczek, “Enforced electrical neutrality of the color-flavor locked phase,” *Phys. Rev. Lett.* **86** (2001) 3492–3495, [arXiv:hep-ph/0012039](#).

- [191] K. Iida and G. Baym, “The superfluid phases of quark matter: Ginzburg-Landau theory and color neutrality,” *Phys. Rev.* **D63** (2001) 074018, [arXiv:hep-ph/0011229](#).
- [192] T. Hatsuda, M. Tachibana, N. Yamamoto, and G. Baym, “New critical point induced by the axial anomaly in dense QCD,” *Phys. Rev. Lett.* **97** (2006) 122001, [arXiv:hep-ph/0605018](#).
- [193] T. Schafer and F. Wilczek, “Continuity of quark and hadron matter,” *Phys. Rev. Lett.* **82** (1999) 3956–3959, [arXiv:hep-ph/9811473](#).
- [194] N. Yamamoto, M. Tachibana, T. Hatsuda, and G. Baym, “Phase structure, collective modes, and the axial anomaly in dense QCD,” *Phys. Rev.* **D76** (2007) 074001, [arXiv:0704.2654 \[hep-ph\]](#).
- [195] N. Yamamoto, “Instanton-induced crossover in dense QCD,” *JHEP* **12** (2008) 060, [arXiv:0810.2293 \[hep-ph\]](#).
- [196] H. Abuki, G. Baym, T. Hatsuda, and N. Yamamoto, “The NJL model of dense three-flavor matter with axial anomaly: the low temperature critical point and BEC-BCS diquark crossover,” *Phys. Rev.* **D81** (2010) 125010, [arXiv:1003.0408 \[hep-ph\]](#).
- [197] R. Casalbuoni and R. Gatto, “Effective theory for color-flavor locking in high density QCD,” *Phys. Lett.* **B464** (1999) 111–116, [arXiv:hep-ph/9908227](#).
- [198] D. T. Son and M. A. Stephanov, “Inverse meson mass ordering in color-flavor-locking phase of high density QCD,” *Phys. Rev.* **D61** (2000) 074012, [arXiv:hep-ph/9910491](#).
- [199] D. T. Son and M. A. Stephanov, “Inverse meson mass ordering in color-flavor-locking phase of high density QCD: Erratum,” *Phys. Rev.* **D62** (2000) 059902, [arXiv:hep-ph/0004095](#).
- [200] P. F. Bedaque and T. Schafer, “High density quark matter under stress,” *Nucl. Phys.* **A697** (2002) 802–822, [arXiv:hep-ph/0105150](#).
- [201] D. B. Kaplan and S. Reddy, “Novel phases and transitions in quark matter,” *Phys. Rev.* **D65** (2002) 054042, [arXiv:hep-ph/0107265](#).
- [202] A. Kryjevski, D. B. Kaplan, and T. Schafer, “New phases in CFL quark matter,” *Phys. Rev.* **D71** (2005) 034004, [arXiv:hep-ph/0404290](#).
- [203] H. Basler and M. Buballa, “NJL model of homogeneous neutral quark matter: Pseudoscalar diquark condensates revisited,” *Phys. Rev.* **D81** (2010) 054033, [arXiv:0912.3411 \[hep-ph\]](#).
- [204] M. M. Forbes, “Kaon condensation in an NJL model at high density,” *Phys. Rev.* **D72** (2005) 094032, [arXiv:hep-ph/0411001](#).
- [205] H. J. Warringa, “The phase diagram of neutral quark matter with pseudoscalar condensates in the color-flavor locked phase,” [arXiv:hep-ph/0606063](#).
- [206] T. Hatsuda, M. Tachibana, and N. Yamamoto, “Spectral continuity in dense QCD,” *Phys. Rev.* **D78** (2008) 011501, [arXiv:0802.4143 \[hep-ph\]](#).
- [207] T. Takatsuka, R. Tamagaki, and T. Tatsumi, “Characteristic aspects of pion condensed phases,” *Prog. Theor. Phys. Suppl.* **112** (1993) 67–106.
- [208] G. Gruner, “The dynamics of charge-density waves,” *Rev. Mod. Phys.* **60** (1988) 1129–1181.
- [209] G. Gruner, “The dynamics of spin-density waves,” *Rev. Mod. Phys.* **66** (1994) 1–24.
- [210] D. V. Deryagin, D. Y. Grigoriev, and V. A. Rubakov, “Standing wave ground state in high density, zero temperature QCD at large N_c ,” *Int. J. Mod. Phys.* **A7** (1992) 659–681.
- [211] E. Shuster and D. T. Son, “On finite-density QCD at large N_c ,” *Nucl. Phys.* **B573** (2000) 434–446, [arXiv:hep-ph/9905448](#).
- [212] E. Nakano and T. Tatsumi, “Chiral symmetry and density wave in quark matter,” *Phys. Rev.* **D71** (2005) 114006, [arXiv:hep-ph/0411350](#).
- [213] V. Schon and M. Thies, “2D model field theories at finite temperature and density,” [arXiv:hep-th/0008175](#).
- [214] T. Kojo, Y. Hidaka, L. McLerran, and R. D. Pisarski, “Quarkyonic chiral spirals,” [arXiv:0912.3800 \[hep-ph\]](#).
- [215] D. Nickel, “How many phases meet at the chiral critical point?,” *Phys. Rev. Lett.* **103** (2009) 072301, [arXiv:0902.1778 \[hep-ph\]](#).
- [216] W. V. Liu and F. Wilczek, “Interior gap superfluidity,” *Phys. Rev. Lett.* **90** (2003) 047002, [arXiv:cond-mat/0208052](#).
- [217] E. Gubankova, W. V. Liu, and F. Wilczek, “Breached pairing superfluidity: Possible realization in QCD,” *Phys. Rev. Lett.* **91** (2003) 032001, [arXiv:hep-ph/0304016](#).
- [218] I. Shovkovy and M. Huang, “Gapless two-flavor color superconductor,” *Phys. Lett.* **B564** (2003) 205, [arXiv:hep-ph/0302142](#).
- [219] M. Huang and I. Shovkovy, “Gapless color superconductivity at zero and at finite temperature,” *Nucl. Phys.* **A729** (2003) 835–863, [arXiv:hep-ph/0307273](#).
- [220] M. Alford, C. Kouvaris, and K. Rajagopal, “Gapless color-flavor-locked quark matter,” *Phys. Rev. Lett.* **92** (2004) 222001, [arXiv:hep-ph/0311286](#).

- [221] M. Alford, C. Kouvaris, and K. Rajagopal, “Evaluating the gapless color-flavor locked phase,” *Phys. Rev.* **D71** (2005) 054009, [arXiv:hep-ph/0406137](#).
- [222] M. Huang and I. A. Shovkovy, “Chromomagnetic instability in dense quark matter,” *Phys. Rev.* **D70** (2004) 051501, [arXiv:hep-ph/0407049](#).
- [223] M. Huang and I. A. Shovkovy, “Screening masses in neutral two-flavor color superconductor,” *Phys. Rev.* **D70** (2004) 094030, [arXiv:hep-ph/0408268](#).
- [224] R. Casalbuoni, R. Gatto, M. Mannarelli, G. Nardulli, and M. Ruggieri, “Meissner masses in the gCFL phase of QCD,” *Phys. Lett.* **B605** (2005) 362–368, [arXiv:hep-ph/0410401](#).
- [225] M. Alford and Q.-h. Wang, “Photons in gapless color-flavor-locked quark matter,” *J. Phys.* **G31** (2005) 719–738, [arXiv:hep-ph/0501078](#).
- [226] K. Fukushima, “Analytical and numerical evaluation of the Debye and Meissner masses in dense neutral three-flavor quark matter,” *Phys. Rev.* **D72** (2005) 074002, [arXiv:hep-ph/0506080](#).
- [227] K. Fukushima, “Phase structure and instability problem in color superconductivity,” [arXiv:hep-ph/0510299](#).
- [228] I. Giannakis and H.-C. Ren, “Chromomagnetic instability and the LOFF state in a two flavor color superconductor,” *Phys. Lett.* **B611** (2005) 137–146, [arXiv:hep-ph/0412015](#).
- [229] K. Fukushima, “Characterizing the Larkin-Ovchinnikov-Fulde-Ferrel phase induced by the chromomagnetic instability,” *Phys. Rev.* **D73** (2006) 094016, [arXiv:hep-ph/0603216](#).
- [230] E. V. Gorbar, M. Hashimoto, and V. A. Miransky, “Neutral LOFF state and chromomagnetic instability in two-flavor dense QCD,” *Phys. Rev. Lett.* **96** (2006) 022005, [arXiv:hep-ph/0509334](#).
- [231] I. Giannakis and H.-C. Ren, “The Meissner effect in a two flavor LOFF color superconductor,” *Nucl. Phys.* **B723** (2005) 255–280, [arXiv:hep-th/0504053](#).
- [232] M. Ciminale, G. Nardulli, M. Ruggieri, and R. Gatto, “Chromomagnetic stability of the three flavor Larkin-Ovchinnikov-Fulde-Ferrell phase of QCD,” *Phys. Lett.* **B636** (2006) 317–323, [arXiv:hep-ph/0602180](#).
- [233] R. Casalbuoni, R. Gatto, N. Ippolito, G. Nardulli, and M. Ruggieri, “Ginzburg-Landau approach to the three flavor LOFF phase of QCD,” *Phys. Lett.* **B627** (2005) 89–96, [arXiv:hep-ph/0507247](#).
- [234] K. Rajagopal and R. Sharma, “The crystallography of three-flavor quark matter,” *Phys. Rev.* **D74** (2006) 094019, [arXiv:hep-ph/0605316](#).
- [235] D. Nickel and M. Buballa, “Solitonic ground states in (color-) superconductivity,” *Phys. Rev.* **D79** (2009) 054009, [arXiv:0811.2400 \[hep-ph\]](#).
- [236] E. V. Gorbar, M. Hashimoto, and V. A. Miransky, “Gluonic phase in neutral two-flavor dense QCD,” *Phys. Lett.* **B632** (2006) 305–312, [arXiv:hep-ph/0507303](#).
- [237] M. Hashimoto and V. A. Miransky, “Gluonic phases and phase diagram in neutral two flavor dense QCD,” *Prog. Theor. Phys.* **118** (2007) 303–314, [arXiv:0705.2399 \[hep-ph\]](#).
- [238] O. Kiriya, D. H. Rischke, and I. A. Shovkovy, “Gluonic phase versus LOFF phase in two-flavor quark matter,” *Phys. Lett.* **B643** (2006) 331–335, [arXiv:hep-ph/0606030](#).
- [239] M. Hashimoto, “Is gluonic color-spin locked phase stable?,” *Phys. Rev.* **D78** (2008) 031501, [arXiv:0803.0175 \[hep-ph\]](#).
- [240] E. J. Ferrer and V. de la Incera, “Chromomagnetic instability and induced magnetic field in neutral two-flavor color superconductivity,” *Phys. Rev.* **D76** (2007) 114012, [arXiv:0705.2403 \[hep-ph\]](#).
- [241] T. Schafer, “Meson supercurrent state in high density QCD,” *Phys. Rev. Lett.* **96** (2006) 012305, [arXiv:hep-ph/0508190](#).
- [242] M. Huang, “Spontaneous current generation in the 2SC phase,” *Phys. Rev.* **D73** (2006) 045007, [arXiv:hep-ph/0504235](#).
- [243] S. Reddy and G. Rupak, “Phase structure of 2-flavor quark matter: Heterogeneous superconductors,” *Phys. Rev.* **C71** (2005) 025201, [arXiv:nucl-th/0405054](#).
- [244] K. Iida and K. Fukushima, “Instability of a gapless color superconductor with respect to inhomogeneous fluctuations,” *Phys. Rev.* **D74** (2006) 074020, [arXiv:hep-ph/0603179](#).
- [245] J. B. Kogut, M. A. Stephanov, and D. Toublan, “On two-color QCD with baryon chemical potential,” *Phys. Lett.* **B464** (1999) 183–191, [arXiv:hep-ph/9906346](#).
- [246] J. B. Kogut, M. A. Stephanov, D. Toublan, J. J. M. Verbaarschot, and A. Zhitnitsky, “QCD-like theories at finite baryon density,” *Nucl. Phys.* **B582** (2000) 477–513, [arXiv:hep-ph/0001171](#).
- [247] A. Nakamura, “Quarks and gluons at finite temperature and density,” *Phys. Lett.* **B149** (1984) 391.
- [248] J. B. Kogut, D. K. Sinclair, S. J. Hands, and S. E. Morrison, “Two-colour QCD at non-zero

- quark-number density,” *Phys. Rev.* **D64** (2001) 094505, [arXiv:hep-lat/0105026](#).
- [249] Y. Nishida, K. Fukushima, and T. Hatsuda, “Thermodynamics of strong coupling 2-color QCD with chiral and diquark condensates,” *Phys. Rept.* **398** (2004) 281–300, [arXiv:hep-ph/0306066](#).
- [250] S. Hands, S. Kim, and J.-I. Skullerud, “Deconfinement in dense 2-color QCD,” *Eur. Phys. J.* **C48** (2006) 193, [arXiv:hep-lat/0604004](#).
- [251] S. Hands, S. Kim, and J.-I. Skullerud, “A quarkyonic phase in dense two color matter?,” *Phys. Rev.* **D81** (2010) 091502, [arXiv:1001.1682 \[hep-lat\]](#).
- [252] T. Brauner, K. Fukushima, and Y. Hidaka, “Two-color quark matter: $U(1)_A$ restoration, superfluidity, and quarkyonic phase,” *Phys. Rev.* **D80** (2009) 074035, [arXiv:0907.4905 \[hep-ph\]](#).
- [253] T. Kanazawa, T. Wettig, and N. Yamamoto, “Chiral Lagrangian and spectral sum rules for dense two-color QCD,” *JHEP* **08** (2009) 003, [arXiv:0906.3579 \[hep-ph\]](#).
- [254] S. Muroya, A. Nakamura, and C. Nonaka, “Behavior of hadrons at finite density: Lattice study of color $SU(2)$ QCD,” *Phys. Lett.* **B551** (2003) 305–310, [arXiv:hep-lat/0211010](#).
- [255] J. B. Kogut, D. Toublan, and D. K. Sinclair, “The pseudo-Goldstone spectrum of 2-colour QCD at finite density,” *Phys. Rev.* **D68** (2003) 054507, [arXiv:hep-lat/0305003](#).
- [256] M.-P. Lombardo, M. L. Paciello, S. Petrarca, and B. Taglienti, “Glueballs and the superfluid phase of two-color QCD,” *Eur. Phys. J.* **C58** (2008) 69–81, [arXiv:0804.4863 \[hep-lat\]](#).
- [257] G. Baym, T. Hatsuda, M. Tachibana, and N. Yamamoto, “The axial anomaly and the phases of dense QCD,” *J. Phys.* **G35** (2008) 104021, [arXiv:0806.2706 \[nucl-th\]](#).
- [258] A. Selem and F. Wilczek, “Hadron systematics and emergent diquarks,” [arXiv:hep-ph/0602128](#).
- [259] K. Maeda, G. Baym, and T. Hatsuda, “Simulating dense QCD matter with ultracold atomic boson-fermion mixtures,” *Phys. Rev. Lett.* **103** (2009) 085301, [arXiv:0904.4372 \[cond-mat.quant-gas\]](#).
- [260] J. J. Zirbel, K.-K. Ni, S. Ospelkaus, T. L. Nicholson, M. L. Olsen, P. S. Julienne, C. E. Wieman, J. Ye, and D. S. Jin, “Heteronuclear molecules in an optical dipole trap,” *Phys. Rev.* **A78** (2008) 013416.
- [261] R. Cherng, G. Refael, and E. Demler, “Superfluidity and magnetism in multicomponent ultracold fermions,” *Phys. Rev. Lett.* **99** (2007) 130406.
- [262] A. Rapp, G. Zaránd, C. Honerkamp, and W. Hofstetter, “Color superfluidity and “Baryon” formation in ultracold fermions,” *Phys. Rev. Lett.* **98** (2007) 160405.
- [263] F. Ozel, G. Baym, and T. Guver, “Astrophysical measurement of the equation of state of neutron star matter,” [arXiv:1002.3153 \[astro-ph.HE\]](#).
- [264] A. W. Steiner, J. M. Lattimer, and E. F. Brown, “The equation of state from observed masses and radii of neutron stars,” [arXiv:1005.0811 \[astro-ph.HE\]](#).
- [265] N. Yasutake, K. Kotake, M.-a. Hashimoto, and S. Yamada, “Effects of QCD phase transition on gravitational radiation from two-dimensional collapse and bounce of massive stars,” *Phys. Rev.* **D75** (2007) 084012, [arXiv:astro-ph/0702476](#).
- [266] K. Sumiyoshi, C. Ishizuka, A. Ohnishi, S. Yamada, and H. Suzuki, “Emergence of hyperons in failed supernovae: trigger of the black hole formation,” *Astrophys. J. Lett.* **690** (2009) L43–L46, [arXiv:0811.4237 \[astro-ph\]](#).
- [267] G. W. Carter and S. Reddy, “Neutrino propagation in color superconducting quark matter,” *Phys. Rev.* **D62** (2000) 103002, [arXiv:hep-ph/0005228](#).